Accepted Manuscript

Design, synthesis and anticancer activity of new monastrol analogues bearing 1,3,4-oxadiazole moiety

Fatma A.F. Ragab, Sahar M. Abou-Seri, Salah A. Abdel-Aziz, Abdallah M. Alfayomy, Mohamed aboelmagd

PII: S0223-5234(17)30472-5

DOI: 10.1016/j.ejmech.2017.06.026

Reference: EJMECH 9521

To appear in: *European Journal of Medicinal Chemistry*

Received Date: 20 March 2017

Revised Date: 1 June 2017

Accepted Date: 14 June 2017

Please cite this article as: F.A.F. Ragab, S.M. Abou-Seri, S.A. Abdel-Aziz, A.M. Alfayomy, M. aboelmagd, Design, synthesis and anticancer activity of new monastrol analogues bearing 1,3,4-oxadiazole moiety, *European Journal of Medicinal Chemistry* (2017), doi: 10.1016/j.ejmech.2017.06.026.

Graphical Abstract

Design, synthesis and anticancer activity of new monastrol analogues bearing 1,3,4-oxadiazole moiety

Fatma A.F. Ragab[1], Sahar M. Abou-Seri[1], Salah A. Abdel-Aziz[2], Abdallah M. Alfayomy[2,*], Mohamed aboelmagd[3,4]

A series of dihydropyrimidines (DHPMs) bearing 1,3,4-oxadiazole moiety were designed and synthesized as monastrol analogues. Compound **9i**, **9k, 9m** and **9n** possessed significant activity against HL-60(TB) and MOLT-4 compared to monastrol.

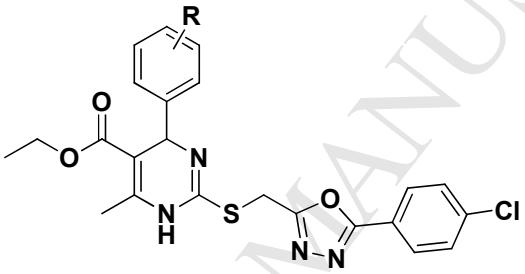

IC50(μM)	HL-60(TB)	MOLT-4
9i: R = 4-Cl	0.103	0.623
9k: R = 4-Br	0.143	0.086
9m: R = 3-Cl	0.056	1.788
9n: R = 2,4-di Cl	0.153	0.080
monastrol	0.147	0.215

Design, synthesis and anticancer activity of new monastrol analogues bearing 1,3,4-oxadiazole moiety

Fatma A.F. Ragab[1], Sahar M. Abou-Seri[1], Salah A. Abdel-Aziz[2], Abdallah M. Alfayomy[2,*], Mohamed Aboelmagd[3,4]

[1]*Department of Pharmaceutical Chemistry, Faculty of Pharmacy, Cairo University, Kasr El-Aini Street, Cairo, P.O. Box, 11562, Egypt*

[2]*Department of Pharmaceutical Chemistry, Faculty of Pharmacy, Al-Azhar University, Assiut, 71524, Egypt*

[3]*National Center for Natural Products Research, School of Pharmacy, The University of Mississippi, University, MS 38677, USA.*

[4]*Pharmacognosy Department, National Research Center, Dokki, Giza, 12622, Egypt*

Abstract

A series of dihydropyrimidine (DHPM) derivatives bearing 1,3,4-oxadiazole moiety was designed and synthesized as monastrol analogues. The new compounds were screened for their cytotoxic activity toward 60 cancer cell lines according to NCI (USA) protocol. Seven compounds were further examined against the most sensitive cell lines, leukemia HL-60(TB) and MOLT-4. The most active compounds were **9m** against HL-60(TB) (IC_{50} = 56 nM) and **9n** against MOLT-4 (IC_{50} = 80 nM), more potent than monastrol (IC_{50} = 147 and 215 nM, respectively). Cell cycle analysis of HL-60(TB) cells treated with **9m** and MOLT-4 cells treated with **9n** showed cell cycle arrest at G2/M phase and pro-apoptotic activity as indicated by annexin V-FITC staining.

Keywords: Dihydropyrimidine, 1,3,4-Oxadiazole, Anticancer activity, Cell cycle arrest, Apoptosis

*Corresponding author: Abdallah M. Alfayomy, E-mail: ph_alfayomy@yahoo.com ; Tel. +201099688027; Fax: +20882181191

1. Introduction

The interest in the anticancer properties of dihydropyrimidines (DHPMs) has been increased since 1999, when monastrol (Fig 1) was discovered. Monastrol is a small molecule that inhibits the motility of the mitotic kinesin Eg5 (motor protein which is required for assembling and maintaining the separation of the half spindles) so inhibits the mitotic machinery and arrests the cells at G2/M phase [1, 2]. When

mitotic arrest is imposed for prolonged periods cells often undergo programmed cell death, known as apoptosis [2]. Drugs that inhibit kinesins are being developed as anticancer agents with the hope that they will inhibit proliferation of tumor cells without having adverse effect on the nervous system. Eg5 inhibitors in general have moderate toxic side effect on the neurons overtime than taxol, a drug commonly used for cancer therapy [3, 4].

However, since the antimitotic activity of monastrol is not very high, attempts to develop more potent and specific inhibitors of kinesin Eg5 based on monastrol scaffold were done [5-8]. Several compounds were synthesized and evaluated for their antitumor activity, among them some compounds showed potent activity such as dimethylenastron [9], vasastrol VS-83 [10], fluorastrol [11], Mon-97 [12]. In addition the Hybrid of DHPM with coumarin which exhibited selective antibreast cancer activity [13] (Fig 1).

(Fig. 1)

Since combination of two or more active structural moieties can possibly augment the bioactivity, so it was of interest to hybridize DHPM nucleus with 1,3,4-oxadiazole fragment through a methylthio bridge hoping to develop potent anticancer agents. The 1,3,4-oxadiazole moiety was chosen as compounds bearing 1,3,4-oxadiazole as zibotentan and compounds **I-III** have been reported to exhibit a significant anticancer activity [14-16] (Fig. 2), hence the incorporation of this moiety in the designed compounds may give new effective antitumor agents.

(Fig. 2)

2. Results and discussion

2.1. Chemistry

The target hybrids have been synthesized by a convergent synthesis including condensation of 6-methyl-4-aryl-1,2,3,4-tetrahydropyrimidine-2(1*H*)-thione derivatives **8a-l** and 2-(chloromethyl)-5-aryl-1,3,4-oxadiazole derivatives **4a-d** (Scheme 1). The reaction occurred by the attack of the more nucleophilic sulfur atom rather than the less nucleophilic nitrogen atom.

scheme 1

The synthetic route for 2-(chloromethyl)-5-aryl-1,3,4-oxadiazole derivatives **4a-d** was illustrated in Scheme 2. Substituted aromatic esters **2a-d** were synthesized by esterification of the corresponding acids **1a-d** with ethanol in the presence of

catalytic amount of sulfuric acid. The synthesized esters **2a-d** were converted to the corresponding acid hydrazides **3a-d** by refluxing with hydrazine hydrate in ethanol [17-20]. Acid hydrazides **3a-d** were cyclized to 2-(chloromethyl)-5-aryl-1,3,4-oxadiazole derivatives **4a-d** through reaction with monochloroacetic acid in phosphorus oxychloride [21, 22].

scheme 2

On the other hand, DHPM derivatives **8a-l** were conveniently prepared via a widely used multicomponent reaction (MCR), of Biginelli type, it involved the cyclocondensation of araldehydes **5**, thiourea **6** and acetylacetone or ethyl acetoacetate **7** in presence of concentrated hydrochloric acid to give the corresponding 6-methyl-4-aryl-1,2,3,4-tetrahydropyrimidine-2(1*H*)-thione derivatives **8a-l** (Scheme 3) [23, 24]. Which were *S*-alkylated with the appropriate 2-(chloromethyl)-5-aryl-1,3,4-oxadiazole derivatives **4a-d** in the presence of triethyl amine and potassium iodide to yield the target compounds **9a-r**.

scheme 3

^{1}H-NMR spectra of compounds **9a-f**, **9h-k**, **9o**, **9q** and **9r** showed an average spectrum in which appeared three singlet signals at δ 10.6-10.9 ppm (N<u>H</u> proton D_2O exchangeable), δ 6.0-6.4 ppm (C4-<u>H</u>) and δ 2.2-2.4 ppm for (C6-C<u>H</u>$_3$). In addition, aromatic protons appeared at δ 6.8-7.9 ppm. Also compounds **9a-f** showed a singlet signal at δ 2.2-2.3 ppm (COC<u>H</u>$_3$) while, compounds **9h-k**, **9o**, **9q** and **9r** showed a characteristic triplet-quartet pattern at δ 0.9-1.2 ppm (CH_2-C<u>H</u>$_3$) and δ 3.9-4.2 ppm (C<u>H</u>$_2$-CH_3). The geminal hydrogens of SC<u>H</u>$_2$ appeared as doublets around 4.36 and 4.45 ppm (J = 17.4 Hz). This was further confirmed by HSQC spectra of compound (**9k**) which showed that these two hydrogens are attached to the carbon appeared at δ 28.90 ppm. This geminal coupling was attributed to the fact that the two hydrogens are diastereomeric protons as a result of the presence of asymmetric center at C4. On the other hand, ^{1}HNMR spectra of compounds **9m** and **9n** revealed the presence of two tautomeric species, 1,4- and 1,6-dihydropyrimidines (Fig. 3), which may be attributed to the effect of the substituent at C4-phenyl ring on tautomerization [25-29]. Similarly ^{1}HNMR spectra of compounds **9g**, **9l** and **9p** in a mixture of DMSO-d_6 and trifluroacetic acid (TFA) revealed separate signals for each tautomeric form. This effect may be due to hindering of the proton transfer process by the formation of H-bonded complexes with the solvent [25, 26].

(Fig. 3)

^{13}CNMR spectra of compounds **9a-f** revealed the presence of carbonyl carbon (ketone) at the range δ 195.53-196.32 ppm while, compounds **9h-k**, **9o**, **9q** and **9r** showed carbonyl carbon (ester) at the range δ 165.02-174.80 ppm. ^{13}CNMR spectra of compound **9n** in DMSO-d_6 and compounds **9g**, **9l**, **9m**, **9p** and **9r** in a mixture of DMSO-d_6 and trifluroacetic acid showed separate signals for each tautomeric form.

2.2. Biological evaluation

2.2.1. ***In vitro*** **cytotoxic screening**

The newly synthesized compounds (**9a-r)** were submitted to Developmental Therapeutic Program-National Cancer Institute, Bethesda, USA (www.dtp.nci.nih.gov) to be screened for their *in vitro* anticancer activity. Thirteen compounds were selected to be evaluated at one dose (10 µM) primary anticancer assay towards a panel of approximately 60 cancer cell lines. The human tumor cell lines were derived from nine different cancer types: leukemia, melanoma, lung, colon, CNS, ovarian, renal, prostate and breast cancers. Screening results for each compound were reported as the percentage growth of the treated cells compared to the untreated control cells and presented as growth inhibition percent (GI%) caused by the test compounds (Table 1).

Table 1

The obtained data revealed that, compounds **9i**, **9k**, **9m** and **9n** showed broad spectrum cytotoxic activity with various degrees of growth inhibition against the tested tumor cell lines. Compounds **9i**, **9k** and **9n** showed potent activity against leukemia cell lines HL-60(TB) and MOLT-4 with GI% ranges of 77.47-106.39 and 88.75-92.98, respectively. Compound **9m** showed potent activity against leukemia HL-60(TB) cell line and non small cell lung cancer NCI-H522 with GI% values 80.42 and 74.59 % respectively. Also compound **9n** showed potent activity against leukemia CCRF-CEM; non small cell lung cancer HOP-92 and colon cancer HCT-116 cell lines with GI% range of 71.24-73.64. In addition, compounds **9i** and **9k** showed moderate activity against leukemia cell lines CCRF-CEM, RPMI-8226, SR; colon cancer HCT-116; melanoma SK-MEL-5; renal cancer UO-31; prostate cancer PC-3; breast cancer MCF-7 and T-47D with GI% range of 47.61-64.22. Moreover compound **9m** showed moderate activity against colon cancer HCT-116 and breast cancer T-47D with GI% values 56.51 and 69.24%, respectively. Compound **9n** showed moderate activity against leukemia SR; CNS cancer SF-295; ovarian cancer IGROV1; renal cancer

RXF 393, UO-31; prostate cancer PC-3; breast cancer MCF-7, MDA-MB-231/ATCC and T-47D with GI% range 52.64-68.03.

It is worth noting that, leukemia HL-60(TB) and MOLT-4 were the most sensitive cancer cell lines to the effect of compounds **9i**, **9k**, **9m** and **9n** with GI% ranges of 77.47-106.39 and 44.97-92.98, respectively (Fig. 4).

(Fig. 4)

2.2.2. *In vitro* IC_{50} evaluation

Compounds **9i**, **9k**, **9l**, **9m, 9n, 9p** and **9r** were further evaluated by determining the median growth inhibitory concentration (IC_{50}) against the most sensitive cell lines, HL-60(TB) and MOLT-4, by the MTT assay using monastrol as a positive control [30]. This permitted a good structure activity relationship study.

Table 2

The results in Table 2 revealed that, the monastrol analogues **9i**, **9k**, **9m** and **9n** which demonstrated the best cytotoxic activity against both cell lines were substituted with ethyl carboxylate function at C5 of DHPM nucleus. In addition, the C4 substituent markedly affected the cytotoxic activity. The most potent derivative against HL-60(TB) cell line was **9m** (IC_{50} = 0.056 µM) bearing a 3-chlorophenyl substituent, showed more inhibitory activity than its congeners **9i** (IC_{50} = 0.103 µM), **9k** (IC_{50} = 0.143 µM) and **9n** (IC_{50} = 0.153 µM) with 4-chlorophenyl, 4-bromophenyl or 2,4-dichlorophenyl substituent, respectively. On the other hand, the most potent derivatives against MOLT-4 were **9n** (IC_{50} = 0.080 µM) and **9k** (IC_{50} = 0.086 µM) having a 2,4-dichlorophenyl or 4-bromophenyl substituent, respectively. While **9i** (IC_{50} = 0.623 µM) and **9m** (IC_{50} = 1.778 µM) with 4-chlorophenyl and 3-chlorophenyl substituents showed good inhibitory activity, this activity was less than **9n** and **9k**. Interestingly, compound **9l** bearing 2-chlorophenyl substituent displayed no activity against both HL-60(TB) and MOLT-4 (IC_{50} = 193 and 255 µM, respectively). Furthermore, the cytotoxic activity was influenced by the C5 substituent at 1,3,4-oxadiazole ring. It was observed that, all the active derivatives **9i**, **9k**, **9m** and **9n** having 4-chlorophenyl substituent. Changing this substituent with phenyl (**9r**) or 4-methylphenyl (**9p**) abolished the activity (IC_{50} of **9r** and **9p** = 74.4 and 220 µM against HL-60(TB) and 344 and 538 µM against MOLT-4).

Finally, comparing the activity of **9i**, **9k**, **9m** and **9n** with the standard drug monastrol against HL60(TB) cell line, compounds **9m** and **9i** were more potent than

monastrol by about 2.5 and 1.5 fold (IC_{50} = 0.056, 0.103 and 0.147 µM, respectively), while compounds **9k** and **9n** were almost equipotent to monastrol (IC_{50} = 0.143 and 0.153 µM, respectively). Regarding MOLT-4 cell line, compounds **9k** and **9n** possessed significant activity which was about 3 times more active than monastrol (IC_{50} = 0.086, 0.080 and 0.215 µM, respectively), while compounds **9i** and **9m** were less active than monastrol (IC_{50} = 0.623 and 1.788 µM, respectively).

To study the effect of lipophilicity on the activity, the log P values were calculated using molinspiration cheminformatics web services [31] and listed in Table 2. It was found that, the active compounds **9i, 9k, 9m** and **9n** showed log P values ranging from 5.51-6.14. The other three inactive compounds **9l, 9p** and **9r** showed log P values ≤ 5.48, which suggest that log P is not a determining factor for cytotoxic activity.

2.2.3. Cell cycle analysis

The effect of compound **9m** on HL-60(TB) cells, **9n** on MOLT-4 cells and monastrol on both cell lines have been studied by flow cytometric analysis. Treatment of HL-60(TB) cells with twice IC_{50} concentration of **9m** (0.112 µM) or of monastrol (0.294 µM) for 24 h resulted in significant alterations in cell cycle phases (Fig. 5). There was a significant increase in the percentage of apoptotic cells at the pre-G phase, (24.72% on exposure to **9m** and 6.89% for monastrol) compared to control (1.43%). Concurrent reduction in the percentage of cells at G0/G1 phase to 32.88% for **9m** and 61.23% for monastrol compared to control (68.43%). Also, a significant increase in the cells at G2/M phase to 14.81% in case of **9m** and 9.98% for monastrol was detected compared to control (7.29%). Similarly, exposure of MOLT-4 cells to 0.160 µM of **9n** (twice IC_{50}) or 0.430 µM of monastrol (twice IC_{50}) for 24 h increased the population of cells at the pre-G phase from 0.88% to 17.83% and 8.63% respectively, whereas G0/G1 cells significantly reduced from 74.22% to 38.52% in case of **9n** and 55.72% in case of monastrol as compared to control. Also, a significant increase in the cells at G2/M phase to 26.61% with **9n** and 13.92% with monastrol compared to control (4.35%). No significant difference was found in the percent of cells in the S phase, (Fig. 6).

Hence, it can be concluded that compounds **9m** and **9n** inhibit the cell proliferation through cell cycle arrest at G2/M phase, which in turn induces cell death by apoptosis. In agreement with the cytotoxicity assay results, apoptosis was more

pronounced in HL-60(TB) and MOLT-4 cells treated with **9m** or **9n** than those treated with monastrol.

(Fig. 5)

(Fig. 6)

2.2.4. Annexin V-FITC apoptosis assay

Further evaluation of the pro-apoptotic effect of compounds **9m** and **9n** was carried out using Annexin V-FITC and propidium iodide double staining. Flow cytometric analysis of the differential binding of the cells to annexin V-FITC and propidium iodide showed a remarkable effect in the proportion of apoptotic cells. HL-60(TB) cells treated with 0.112 µM of **9m** (twice IC_{50}) or 0.294 µM of monastrol (twice IC_{50}) showed an increase in the percent of annexin V-FITC positive apoptotic cells (UR+LR) to 23.76% (19.3 folds) for **9m** and 6.26% (5.1 folds) for monastrol compared to control (1.23%) (Fig. 7). On the other hand MOLT-4 cells treated with 0.160 µM of **9n** (twice IC_{50}) or 0.430 µM of monastrol (twice IC_{50}) showed an increase in the percent of annexin V-FITC positive apoptotic cells (UR+LR) to 16.37% (21 folds) for **9n** and 7.60% (10 folds) for monastrol compared to control (0.77%) (Fig. 8). These results proved that the anti-proliferative effect of compounds **9m** and **9n** is attributed to their potent pro-apoptotic activity and further supported our finding that HL-60(TB) and MOLT-4 cells are more sensitive to the synthesized compounds than to monastrol.

(Fig. 7)

(Fig. 8)

2.2.4. Docking study

It is well known that the monastrol exerts its antitumor activity by inhibition of mitotic kinesin Eg5. Cell cycle analysis of HL-60(TB) and MOLT-4 cells treated with compounds **9m** and **9n** respectively revealed G2/M phase arrest followed by apoptosis similar to monastrol. This observation suggests that kinesin Eg5 could be a potential target for the synthesized monastrol analogues. Therefore a molecular docking study of **9m** and **9n** into the crystal structure of Eg5 motor domain in complex with the allosteric inhibitor monastrol (PDB ID code 1Q0B) [32] was performed using Molecular Operating Environment (MOE version 2008.10) [33]. The most stable docking model was selected according to the best scored conformation predicted by the MOE scoring function. To validate the docking protocol, the co-crystallized ligand was redocked into Eg5 allosteric binding site and the docking pose

was compared with the initial pose using root mean square deviation (RMSD). Monastrol docked almost at the same position (RMSD = 0.837Å) with docking energy score of -11.74 kcal/mol.

Analysis of the molecular docking results showed that, compounds **9m** and **9n** could fit into the allosteric binding site with docking energy scores of -14.73 and -15.76 kcal/mol, respectively (Fig. 9). The DHPM ring occupied the same position as monastrol. The DHPM N-1 showed the potential to be involved in a key H-bond interaction with the main chain carbonyl of Glu116. In addition, the N-3 of DHPM ring formed a water mediated H-bond with Leu214. The substituted chlorophenyl moiety at position 4 of DHPM ring pointed toward the solvent region but maintained hydrophobic interaction with the side chains of Ala218 and/or Tyr211. Unlike monastrol, the 4-chlorophenyl-1,3,4-oxadiazole moiety projected into the core of the protein, where the oxadiazole ring was involved in π...cation interaction with side chain of Arg221, while the 4-chlorophenyl rest occupied a hydrophobic pocket bordered by the side chains of Met115, Ile136, Ser237, Val238, Phe239, Leu263, Val264 and Asp265. Moreover, halogen bonding between the 4-chlorine atom and the main chain carbonyl oxygen of Leu263 (2.82 Å) and Val264 (≤3.5 Å) could justify the importance of 4-chlorophenyl substituent on the oxadiazole for cytotoxic activity

(Fig. 9)

3. Conclusion

Certain new hybrids of DHPM and 1,3,4-oxadiazole have been synthesized as monastrol analogues and investigated for their *in vitro* cytotoxic activity. Compounds **9i**, **9k**, **9m** and **9n** featuring a *p*-chlorophenyl rest on the oxadiazole ring, ethyl carboxylate function at C5 and *m*/*p*-chloro(bromo)phenyl substituent at C4 of DHPM nucleus, showed the highest cytotoxic activity against leukemia HL-60(TB) and MOLT-4 cell lines with IC_{50} ranges = 0.056-0.153 and 0.080-1.788 µm, respectively, which exceed or equipotent to monastrol. Cell cycle analysis of HL-60(TB) cells treated with **9m** and MOLT-4 cells treated with **9n** revealed a significant G2/M phase arrest coupled with an increase in the percentage of cells in pre-G phase, which is indicative of apoptosis. The pro-apoptotic activity of **9m** and **9n** was inferred by the significant increase in the percentage of annexin V-FITC-positive apoptotic cells.

4. Experimental

4.1. Chemistry

Unless otherwise noted, all materials were obtained from commercial suppliers and used without further purification. Reactions were monitored by TLC (Kieselgel 60 F254 precoated plates, E. Merck, Germany), the spots were detected by exposure to UV lamp at λ 254nm. Melting points were determined on an electro thermal melting point apparatus (Stuart Scientific Co.) and were uncorrected. ^{1}HNMR and ^{13}CNMR spectra were determined in DMSO-d_6 and TFA used with some compounds for solubility. NMR instruments are Bruker Avance DRX 500 MHz spectrometer; 3 mm inverse, dual and HPLC flow probes with gradient variable temperature control (vtc), Bruker Avance DRX 400 MHz spectrometer; 3 mm inverse probe, Department of BioMolecular Sciences, the university of Mississippi, USA and BRUKER Avance III 400 MHz NMR spectrometer, Faculty of Pharmacy, Beni-Suif University, Egypt. Chemical shifts δ are reported in parts per million (ppm) downfield from tetramethylsilane (TMS) internal standard. Elemental microanalyses were performed at the Regional Center for Mycology and Biotechnology, Al-Azhar University, Egypt. Infrared Spectra were recorded on Shimadzu-FTIR spectrophotometer, Faculty of Pharmacy, Cairo University, Egypt and expressed in wave number (cm^{-1}), using potassium bromide discs.

Preparation and analytical data of compounds **4a-d** [16, 22] and **8a-l** [8, 23, 34, 35] were as reported.

4.1 Synthesis of compounds 9a-r

A mixture of 6-methyl-5-(ethoxy or methyl)carbonyl-4-(substituted)phenyl-2-thioxo-1,2,3,4-tetrahydropyrimidine **8a-l** (2 mmol), 2-(chloromethyl)-5-(substituted) phenyl-1,3,4-oxadiazole **4a-d** (2 mmol), potassium iodide (2 mmol), and triethyl amine (2.5 mmole), was refluxed for 4h in absolute ethanol (20 ml). The reaction mixture was poured onto crushed ice (40 g), acidified with acetic acid (2 ml). The deposited precipitate was filtered, washed with cold water, dried, and crystallized from methanol/DMF mixture.

4.1.1. 1-(2-(((5-(4-chlorophenyl)-1,3,4-oxadiazol-2-yl)methyl)thio)-6-methyl-4-phenyl-1,4-dihydropyrimidin-5-yl)ethanone (9a).

Yield: 76%; Melting point: 196-198 °C; IR (KBr) ν_{max}/cm^{-1} 3452, 3163, 169o, 1651. ^{1}H NMR (400 MHz, DMSO-d_6) δ 10.83 (s, 1H, N-H), 7.86 (d, J = 8.4 Hz, 2H, Ar-H),

7.56 (d, *J* = 8.4 Hz, 2H, Ar-H), 7.42 (d, *J* = 7.4 Hz, 2H, Ar-H), 7.27 (m, 3H, Ar-H), 6.26 (s, 1H C4-H), 4.45 (d, *J* = 17.5 Hz, 1H, S-CH_2), 4.36 (d, *J* = 17.4 Hz, 1H, S-CH_2), 2.35 (s, 3H, C6-CH_3), 2.25 (s, 3H, CO-CH_3). ^{13}C NMR (100 MHz, DMSO-d_6) δ 195.92, 162.16, 161.91, 154.09, 152.01, 140.28, 136.41, 132.29, 130.04, 128.42, 128.19, 127.98, 115.57, 54.86, 48.64, 30.89, 28.26, 23.77. Anal. Calcd for $C_{22}H_{19}ClN_4O_2S$ (438.93):C, 60.20; H, 4.36; N, 12.76. Found: C, 60.47; H, 4.49; N, 13.02.

4.1.2. 1-(2-(((5-(4-chlorophenyl)-1,3,4-oxadiazol-2-yl)methyl)thio)-4-(4-fluorophenyl)-6-methyl-1,4-dihydropyrimidin-5-yl)ethanone (9b).

Yield: 72%; Melting point: 186-188 °C; IR (KBr) ν_{max}/cm^{-1} 3421, 3170, 1680, 1639. ^{1}H NMR (400 MHz, DMSO-d_6) δ 10.86 (s, 1H, NH), 7.87 (d, *J* = 8.3 Hz, 2H, Ar-H), 7.57 (d, *J* = 8.3 Hz, 2H, Ar-H), 7.48 (dd, *J* = 7.7, 5.8 Hz, 2H, Ar-H), 7.14 (t, *J* = 8.6 Hz, 2H, Ar-H), 6.24 (s, 1H, C4-H), 4.46 (d, *J* = 17.5 Hz, 1H, S-CH_2), 4.37 (d, *J* = 17.4 Hz, 1H, S-CH_2), 2.37 (s, 3H, C6-CH_3), 2.26 (s, 3H, CO-CH_3). ^{13}C NMR (100 MHz, DMSO-d_6+TFA) δ 195.53, 167.00, 163.93, 163.36, 161.48, 148.89, 142.11, 137.32, 134.45, 132.10, 131.80, 131.75, 130.20, 128.76, 115.75, 115.54, 56.05, 31.10, 30.83, 19.10. Anal. Calcd for $C_{22}H_{18}ClFN_4O_2S$ (456.92):C, 57.83; H, 3.97; N, 12.26. Found: C, 58.17; H, 4.48; N, 12.50.

4.1.3. 1-(4-(4-chlorophenyl)-2-(((5-(4-chlorophenyl)-1,3,4-oxadiazol-2-yl)methyl)thio)-6-methyl-1,4-dihydropyrimidin-5-yl)ethanone (9c).

Yield: 83%; Melting point: 198-200 °C; IR (KBr) ν_{max}/cm^{-1} 3371, 3170, 1697, 1660, 1651. ^{1}H NMR (400 MHz, DMSO-d_6) δ 10.85 (s, 1H, NH), 7.86 (d, *J* = 8.3 Hz, 2H, Ar-H), 7.55 (d, *J* = 8.5 Hz, 2H, Ar-H), 7.44 (d, *J* = 8.3 Hz, 2H, Ar-H), 7.36 (d, *J* = 8.3 Hz, 2H, Ar-H), 6.22 (s, 1H, C4-H), 4.45 (d, *J* = 17.4 Hz, 1H, S-CH_2), 4.36 (d, *J* = 17.4 Hz, 1H, S-CH_2), 2.36 (s, 3H, C6-CH_3), 2.26 (s, 3H, CO-CH_3). ^{13}C NMR (100 MHz, DMSO-d_6) δ 196.19, 162.71, 162.44, 154.16, 152.83, 139.58, 136.89, 133.28, 132.60, 130.46, 130.05, 128.88, 128.79, 115.68, 54.79, 31.44, 28.69, 24.33. Anal. Calcd for $C_{22}H_{18}Cl_2N_4O_2S$ (473.37):C, 55.82; H, 3.83; N, 11.84. Found: C, 56.13; H, 3.9o; N, 12.16.

4.1.4. 1-(2-(((5-(4-chlorophenyl)-1,3,4-oxadiazol-2-yl)methyl)thio)-4-(4-methoxyphenyl)-6-methyl-1,4-dihydropyrimidin-5-yl)ethanone (9d).

Yield: 85%; Melting point: 218-220 °C; IR (KBr) ν_{max}/cm^{-1} 3367, 3163, 1693, 1651. ^{1}H NMR (400 MHz, DMSO-d_6) δ 10.83 (s, 1H, NH), 7.85 (d, *J* = 8.1 Hz, 2H, Ar-H),

7.57 (d, *J* = 8.3 Hz, 2H, Ar-H), 7.35 (d, *J* = 8.2 Hz, 2H, Ar-H), 6.86 (d, *J* = 8.4 Hz, 2H, Ar-H), 6.20 (s, 1H, C4-H), 4.43 (d, *J* = 17.5 Hz, 1H, S-CH_2), 4.33 (d, *J* = 17.4 Hz, 1H, S-CH_2), 3.70 (s, 3H, O-CH_3), 2.34 (s, 3H, C6-CH_3), 2.22 (s, 3H, CO-CH_3). ^{13}C NMR (100 MHz, DMSO-d_6) δ 196.32, 162.79, 162.09, 159.52, 154.39, 152.15, 136.85, 132.70, 132.63, 130.05, 129.97, 128.93, 115.88, 114.12, 55.51, 54.78, 31.14, 28.58, 24.09. Anal. Calcd for $C_{23}H_{21}ClN_4O_3S$ (468.96):C, 58.91; H, 4.51; N, 11.95. Found: C, 59.12; H, 4.39; N, 12.21.

4.1.5. 1-(4-(4-fluorophenyl)-2-(((5-(4-methoxyphenyl)-1,3,4-oxadiazol-2-yl)methyl)thio)-6-methyl-1,4-dihydropyrimidin-5-yl)ethanone (9e).

Yield: 65%; Melting point: 210-212 °C; IR (KBr) ν_{max}/cm^{-1} 3394, 5178, 1693,1658. ^{1}H NMR (400 MHz, DMSO-d_6) δ 10.64 (s, 1H, NH), 7.82 (d, *J* = 8.7 Hz, 2H, Ar-H), 7.47 (t, *J* = 8.9 Hz, 2H, Ar-H), 7.14 (t, *J* = 8.9 Hz, 2H, Ar-H), 7.03 (d, *J* = 8.4 Hz, 2H, Ar-H), 6.24 (s, 1H, C4-H), 4.46 (d, *J* = 17.3 Hz, 1H, S-CH_2), 4.36 (d, *J* = 17.4 Hz, 1H, S-CH_2), 3.82 (s, 3H, O-CH_3), 2.37 (s, 3H, C6-CH_3), 2.26 (s, 3H, CO-CH_3). ^{13}C NMR (100 MHz, DMSO-d_6) δ 196.25, 163.42, 163.24, 162.38, 162.33, 160.99, 152.82, 136.99, 130.70, 130.67, 130.02, 125.94, 115.73, 115.68, 115.46, 114.04, 55.86, 54.58, 31.37, 28.60, 24.28. Anal. Calcd for $C_{23}H_{21}FN_4O_3S$ (452.50):C, 61.05; H, 4.68; N, 12.38. Found: C, 60.89; H, 4.76; N, 12.70.

4.1.6. 1-(4-(4-fluorophenyl)-6-methyl-2-(((5-(p-tolyl)-1,3,4-oxadiazol-2-yl)methyl)thio)-1,4-dihydropyrimidin-5-yl)ethanone (9f).

Yield: 70%; Melting point: 184-186 °C; IR (KBr) ν_{max}/cm^{-1} 3417, 3170, 169o, 1670, 1643**.** ^{1}H NMR (400 MHz, DMSO-d_6) δ 10.71 (s, 1H, NH), 7.76 (d, *J* = 7.6 Hz, 2H, Ar-H), 7.49 (t, 2H, *J* = 7.6 Hz, Ar-H), 7.30 (d, *J* = 8.0 Hz, 2H, Ar-H), 7.14 (t, *J* = 8.6 Hz, 2H, Ar-H), 6.26 (s, 1H, C4-H), 4.47 (d, *J* = 17.4 Hz, 1H, S-CH_2), 4.36 (d, *J* = 17.4 Hz, 1H, S-CH_2), 2.37 and 2.36 (2s, 6H, C6-CH_3, Ar-CH_3), 2.26 (s, 3H, CO-CH_3). ^{13}C NMR (100 MHz, DMSO-d_6) δ 196.24, 163.63, 163.43, 162.37, 161.00, 153.67, 152.83, 142.05, 136.97, 131.03, 130.79, 130.71, 129.33, 128.14, 115.68, 115.47, 54.58, 31.38, 28.62, 24.30, 21.47. Anal. Calcd for $C_{23}H_{21}FN_4O_2S$ (436.50):C, 63.29; H, 4.85; N, 12.84. Found: C, 63.14; H, 4.99; N, 13.17.

4.1.7. Ethyl 2-(((5-(4-chlorophenyl)-1,3,4-oxadiazol-2-yl)methyl)thio)-6-methyl-4-phenyl-1,4-dihydropyrimidine-5-carboxylate (9g).

Yield: 83%; Melting point: 190-192 °C; IR (KBr) ν_{max}/cm^{-1} 3417, 3178,1720, 1697, 1651. ^{1}H NMR (400 MHz, DMSO-d_6+TFA) δ 10.21 and 9.11 (2s, 1H, NH,), 7.89-

7.20 (m, 9H, Ar-H), 6.26 and 5.59 (2s, 1H, C4-H), 5.06– 4.55 (m, 2H, S-CH_2), 4.17-3.92 (m, 2H, CH_2-CH_3), 2.43 and 2.23 (2s, 3H, C6-CH_3), 1.19-1.04 (m, 3H, CH_2-CH_3). ^{13}C NMR (100 MHz, DMSO-d6+TFA) δ 165.77, 165.60, 152.70, 148.53, 145.25, 138.35, 129.87, 129.20, 128.80, 128.67, 127.59, 126.67, 99.89, 61.10, 59.54, 54.49, 17.99, 14.11, 13.86. Anal. Calcd for $C_{23}H_{21}ClN_4O_3S$ (468.96):C, 58.91; H, 4.51; N, 11.95. Found: C, 59.20; H, 4.57; N, 12.23.

4.1.8. Ethyl 2-(((5-(4-chlorophenyl)-1,3,4-oxadiazol-2-yl)methyl)thio)-4-(4-fluorophenyl)-6-methyl-1,4-dihydropyrimidine-5-carboxylate (9h).

Yield: 84%; Melting point: 210-212 °C; IR (KBr) ν_{max}/cm^{-1} 3394, 3178, 1708, 1693, 1651. ^{1}H NMR (400 MHz, DMSO-d_6) δ 10.81 (s, 1H, NH), 7.85 (d, J = 8.4 Hz, 2H, Ar-H), 7.57 (d, J = 8.4 Hz, 2H, Ar-H), 7.44 (dd, J = 8.0, 5.7 Hz, 2H, Ar-H), 7.14 (t, J = 8.7 Hz, 2H, Ar-H), 6.12 (s, 1H, C4-H), 4.45 (d, J = 17.5 Hz, 1H, S-CH_2), 4.35 (d, J = 17.4 Hz, 1H, S-CH_2), 4.02 (q, J = 7.1 Hz, 2H, CH_2-CH_3), 2.34 (s, 3H, C6-CH_3), 1.11 (t, J = 7.1 Hz, 3H, CH_2-CH_3). ^{13}C NMR (100 MHz, DMSO-d_6) δ 165.53, 162.59, 162.54, 154.21, 153.80, 137.34, 136.83, 132.65, 130.59, 130.51, 130.03, 128.89, 115.65, 115.44, 106.10, 60.27, 54.98, 28.58, 23.05, 14.44. Anal. Calcd for $C_{23}H_{20}ClFN_4O_3S$ (486.95):C, 56.73; H, 4.14; N, 11.51. Found: C, 57.01; H, 4.23; N, 11.84.

4.1.9. Ethyl 4-(4-chlorophenyl)-2-(((5-(4-chlorophenyl)-1,3,4-oxadiazol-2-yl)methyl)thio)-6-methyl-1,4-dihydropyrimidine-5-carboxylate (9i).

Yield: 80%; Melting point: 204-206 °C; IR (KBr) ν_{max}/cm^{-1} 3402, 3174, 1708, 1693, 1651. ^{1}H NMR (400 MHz, DMSO-d_6) δ 10.82 (s, 1H, NH), 7.85 (d, J = 8.3 Hz, 2H, Ar-H), 7.57 (d, J = 8.4 Hz, 2H, Ar-H), 7.41 (dd, J = 8.8, 8.4 Hz, 4H, Ar-H), 6.10 (s, 1H, C_4-H), 4.46 (d, J = 17.4 Hz, 1H, S-CH_2), 4.36 (d, J = 17.4 Hz, 1H, S-CH_2), 4.03 (q, J = 5.2 Hz, 2H, CH_2-CH_3), 2.34 (s, 3H, , C6-CH_3), 1.12 (t, J = 7.1 Hz, 3H, CH_2-CH_3). ^{13}C NMR (100 MHz, DMSO-d_6) δ 165.02, 162.17, 153.72, 153.44, 139.52, 136.36, 132.78, 132.16, 129.82, 129.55, 128.41, 128.30, 105.37, 59.85, 54.69, 28.11, 22.66, 13.97. Anal. Calcd for $C_{23}H_{20}Cl_2N_4O_3S$ (503.40):C, 54.88; H, 4.00; N, 11.13. Found: C, 55.13; H, 3.94; N, 11.36.

4.1.10. Ethyl 2-(((5-(4-chlorophenyl)-1,3,4-oxadiazol-2-yl)methyl)thio)-4-(4-methoxyphenyl)-6-methyl-1,4-dihydropyrimidine-5-carboxylate (9j).

Yield: 62%; Melting point: 208-210 °C; IR (KBr) ν_{max}/cm^{-1} 3394, 3174, 1715, 1693, 1647. ^{1}H NMR (400 MHz, DMSO-d_6) δ 10.79 (s, 1H, NH), 7.85 (d, J = 8.0 Hz, 2H,

Ar-H), 7.58 (d, *J* = 8.1 Hz, 2H, Ar-H), 7.32 (d, *J* = 8.0 Hz, 2H, Ar-H), 6.87 (d, *J* = 8.1 Hz, 2H, Ar-H), 6.09 (s, 1H, C4-H), 4.44 (d, *J* = 17.3 Hz, 1H, S-CH_2), 4.35 (d, *J* = 17.2 Hz, 1H, S-CH_2), 4.03 (q, 2H, *J* = 4 Hz CH_2-CH_3), 3.71 (s, 3H, OCH_3), 2.34 (s, 3H, C6-CH_3), 1.13 (t, *J* = 7.1 Hz, 3H, CH_2-CH_3). Anal. Calcd for $C_{24}H_{23}ClN_4O_4S$ (498.98):C, 57.77; H, 4.65; N, 11.23. Found: C, 58.04; H, 4.79; N, 11.58.

4.1.11. Ethyl 4-(4-bromophenyl)-2-(((5-(4-chlorophenyl)-1,3,4-oxadiazol-2-yl)methyl)thio)-6-methyl-1,4-dihydropyrimidine-5-carboxylate (9k).

Yield: 83%; Melting point: 190-192 °C; IR (KBr) ν_{max}/cm^{-1} 3402, 3170, 1712, 1693, 1651. ^{1}H NMR (400 MHz, DMSO-d_6) δ 10.82 (s, 1H, NH), 7.84 (d, *J* = 8.3 Hz, 2H, Ar-H), 7.58 (d, *J* = 8.3 Hz, 2H, Ar-H), 7.53 (d, *J* = 8.1 Hz, 2H, Ar-H), 7.35 (d, *J* = 8.1 Hz, 2H, Ar-H), 6.09 (s, 1H, C4-H), 4.45 (d, *J* = 17.4 Hz, 1H, S-CH_2), 4.35 (d, *J* = 17.4 Hz, 1H, S-CH_2), 4.04 (q, *J* = 3.6 Hz, 2H, CH_2-CH_3), 2.34 (s, 3H, C6-CH_3), 1.13 (t, *J* = 7.1 Hz, 3H, CH_2-CH_3). ^{13}C NMR (100 MHz, DMSO-d_6) δ 165.49, 162.69, 162.59, 154.17, 153.91, 140.40, 136.82, 132.63, 131.72, 130.60, 130.04, 128.90, 121.90, 105.77, 60.36, 55.22, 28.60, 23.10, 14.46. Anal. Calcd for $C_{23}H_{20}BrClN_4O_3S$ (547.85):C, 50.42; H, 3.68; N, 10.23. Found: C, 50.35; H, 3.81; N, 10.59.

4.1.12. Ethyl 4-(2-chlorophenyl)-2-(((5-(4-chlorophenyl)-1,3,4-oxadiazol-2-yl)methyl)thio)-6-methyl-1,4-dihydropyrimidine-5-carboxylate (9l).

Yield: 85%; Melting point: 194-196 °C; IR (KBr) ν_{max}/cm^{-1} 3417, 3167,1716, 1693,1658. ^{1}H NMR (500 MHz, DMSO-d_6) δ 10.73 and 9.82 (2s, 1H, NH), 7.82-7.06 (m, 8H, Ar-H), 6.38, 5.84 and 5.76 (3s, 1H, C4-H), 4.55-4.27 (m, 2H, S-CH_2), 4.09-3.85 (m, 2H, CH_2-CH_3), 2.29 and 2.26 (2s, 3H, C6-CH_3), 1.13-0.85 (m, 3H, CH_2-CH_3). ^{13}C NMR (100 MHz, DMSO-d_6) δ 174.80, 165.43, 160.54, 157.54, 141.42, 137.66, 137.50, 130.79, 130.48, 130.02, 129.56, 128.99, 128.56, 128.35, 127.96, 127.71, 121.93, 105.18, 78.30, 61.10, 59.53, 58.54, 57.57, 25.43, 16.87, 16.58, 13.46, 13.31. Anal. Calcd for $C_{23}H_{20}Cl_2N_4O_3S$ (503.40):C, 54.88; H, 4.00; N, 11.13. Found: C, 55.12; H, 3.87; N, 11.40.

4.1.13. Ethyl 4-(3-chlorophenyl)-2-(((5-(4-chlorophenyl)-1,3,4-oxadiazol-2-yl)methyl)thio)-6-methyl-1,4-dihydropyrimidine-5-carboxylate (9m).

Yield: 88%; Melting point: 184-186 °C; IR (KBr) ν_{max}/cm^{-1} 3417, 3167, 1716, 1693, 1654. ^{1}H NMR (400 MHz, DMSO-d_6) δ 10.72 and 9.82 (2s, 1H, NH), 7.82-7.12 (m, 8H, Ar-H), 6.38 and 5.85 (2s, 1H, C4-H), 4.55-4.26 (m, 2H, S-CH_2), 4.02-3.85 (m, 2H, CH_2-CH_3), 2.30 and 2.26 (2s, 3H, C6-CH_3), 1.13-0.95 (m, 3H, CH_2-CH_3). ^{13}C

NMR (125 MHz, DMSO-d_6+TFA) δ 165.61, 165.33, 164.26, 163.65, 162.21, 160.50, 152.14, 149.19, 141.76, 132.20, 129.99, 129.65, 129.13, 128.99, 128.29, 127.69, 122.05, 105.19, 98.52, 61.02, 59.36, 52.93, 52.02, 25.52, 17.62, 16.64, 13.57. Anal. Calcd for $C_{23}H_{20}Cl_2N_4O_3S$ (503.40):C, 54.88; H, 4.00; N, 11.13. Found: C, 55.08; H, 4.04; N, 11.34.

4.1.14. Ethyl 2-(((5-(4-chlorophenyl)-1,3,4-oxadiazol-2-yl)methyl)thio)-4-(2,4-dichlorophenyl)-6-methyl-1,4-dihydropyrimidine-5-carboxylate (9n).

Yield: 80%; Melting point: 148-150 °C; IR (KBr) ν_{max}/cm^{-1} 3394, 3178, 1689, 1658. ^{1}H NMR (400 MHz, DMSO-d_6) δ 10.74 and 9.91 (2s, 1H NH), 7.83-7.11 (m, 7H, Ar-H), 6.33 and 5.78 (2s, 1H, C4-H), 4.57-4.28 (m, 2H, S-CH$_2$), 4.23-3.85 (m, 2H, CH$_2$-CH$_3$), 2.29 and 2.27 (2s, 3H, C6-CH$_3$), 1.13-0.95 (m, 3H, CH$_2$-CH$_3$). ^{13}C NMR (100 MHz, DMSO-d_6) δ 165.97, 165.42, 164.79, 163.15, 162.61, 162.06, 155.17, 153.49, 141.49, 137.35, 136.97, 136.78, 133.99, 133.78, 132.79, 132.59, 130.40, 130.00, 129.91, 129.56, 128.83, 128.30, 128.01, 127.58, 122.53, 104.61, 60.27, 59.54, 56.52, 54.96, 28.21, 23.78, 23.07, 17.82, 14.46, 14.36. Anal. Calcd for $C_{23}H_{19}Cl_3N_4O_3S$ (537.85):C, 51.36; H, 3.56; N, 10.42. Found: C, 51.80; H, 3.67; N, 10.75.

4.1.15. Ethyl 4-(4-fluorophenyl)-2-(((5-(4-methoxyphenyl)-1,3,4-oxadiazol-2-yl)methyl)thio)-6-methyl-1,4-dihydropyrimidine-5-carboxylate (9o).

Yield: 95%; Melting point: 220-222°C; IR (KBr) ν_{max}/cm^{-1} 3390, 3178, 1693, 1654. ^{1}H NMR (400 MHz, DMSO-d_6) δ 10.60 (s, 1H, NH), 7.81 (d, J = 8.7 Hz, 2H, Ar-H), 7.44 (t, J = 7.7 Hz, 2H, Ar-H), 7.15 (t, J = 7.7 Hz, 2H, Ar-H), 7.03 (d, J = 8.7 Hz, 2H, Ar-H), 6.13 (s, 1H, C4-H), 4.45 (d, J = 17.4 Hz, 1H, S-CH$_2$), 4.35 (d, J = 17.3 Hz, 1H, S-CH$_2$), 4.03 (q, J = 7.1 Hz, 2H, CH$_2$-CH$_3$), 3.82 (s, 3H, OCH$_3$), 2.34 (s, 3H, C6-CH$_3$), 1.11 (t, J = 7.1 Hz, 3H, CH$_2$-CH$_3$). ^{13}C NMR (125 MHz, DMSO-d_6) δ 165.59, 163.23, 163.20, 162.65, 153.92, 153.58, 130.57, 130.50, 130.03, 125.90, 115.64, 115.47, 114.05, 105.95, 60.28, 55.87, 54.89, 28.56, 23.06, 14.45. Anal. Calcd for $C_{24}H_{23}FN_4O_4S$ (482.53):C, 59.74; H, 4.80; N, 11.61. Found: C, 60.02; H, 4.89; N, 11.87.

4.1.16. Ethyl 4-(4-chlorophenyl)-6-methyl-2-(((5-(p-tolyl)-1,3,4-oxadiazol-2-yl)methyl)thio)-1,4-dihydropyrimidine-5-carboxylate (9p).

Yield: 79%; Melting point: 194-196 °C; IR (KBr) ν_{max}/cm^{-1} 3367, 3178, 1715, 1693,1651. ^{1}H NMR (400 MHz, DMSO-d_6+TFA) δ 8.25 (s, 1H, NH), 7.65-7.09 (m, 8H, Ar-H), 6.27 and 5.54 (2s, 1H, C4-H), 4.68-4.44 (m, 2H, S-CH$_2$), 3.93 (m, 2H,

C<u>H</u>$_2$-CH$_3$), 2.37 and 2.33 (2s, 3H, C6-C<u>H</u>$_3$), 2.24 and 2.26 (2s, 3H, Ar-C<u>H</u>$_3$), 1.01-0.97 (m, 3H, CH$_2$-C<u>H</u>$_3$). ^{13}C NMR (100 MHz, DMSO-d_6+TFA) δ 168.44, 166.68, 165.50, 163.96, 162.10, 153.12, 148.02, 143.75, 143.56, 143.08, 139.07, 134.19, 132.63, 129.84, 129.55, 129.29, 129.01, 128.94, 128.68, 128.46, 128.38, 127.78, 127.61, 126.60, 105.51, 100.03, 60.84, 59.62, 54.70, 54.16, 33.54, 20.61, 17.61, 16.62, 13.48, 13.25. Anal. Calcd for $C_{24}H_{23}ClN_4O_3S$ (482.98):C, 59.68; H, 4.80; N, 11.60. Found: C, 59.91; H, 4.87; N, 11.89.

4.1.17. Ethyl 4-(4-fluorophenyl)-6-methyl-2-(((5-(p-tolyl)-1,3,4-oxadiazol-2-yl)methyl)thio)-1,4-dihydropyrimidine-5-carboxylate (9q).

Yield: 74%; Melting point: 202-204 °C; IR (KBr) ν_{max}/cm^{-1} 3387, 3186, 1715, 1693, 1651. ^{1}H NMR (400 MHz, DMSO-d_6) δ 10.66 (s, 1H, N<u>H</u>), 7.74 (d, *J* = 7.5 Hz, 2H, Ar-<u>H</u>), 7.45 (dd, , *J* = 8, 4,9 Hz, 2H, Ar-<u>H</u>), 7.30 (d, *J* = 7.9 Hz, 2H, Ar-<u>H</u>), 7.15 (t, *J* = 8.4 Hz, 2H, Ar-<u>H</u>), 6.14 (s, 1H, C4-<u>H</u>), 4.46 (d, *J* = 17.4 Hz, 1H, S-C<u>H</u>$_2$), 4.35 (d, *J* = 17.4 Hz, 1H, S-C<u>H</u>$_2$), 4.03 (q, *J* = 6 Hz, 2H, C<u>H</u>$_2$-CH$_3$), 2.36, 2.35 (2s, 6H, C6-C<u>H</u>$_3$, Ar-C<u>H</u>$_3$), 1.12 (t, *J* = 7.1 Hz, 3H, CH$_2$ C<u>H</u>$_3$). ^{13}C NMR (100 MHz, DMSO-d_6) δ 165.57, 163.54, 162.59, 161.02, 153.87, 153.74, 142.01, 137.41, 131.03, 130.59, 130.52, 129.31, 128.12, 115.64, 115.42, 106.02, 60.27, 54.96, 28.53, 23.06, 21.46, 14.44. Anal. Calcd for $C_{24}H_{23}FN_4O_3S$ (466.53):C, 61.79; H, 4.97; N, 12.01. Found: C, 62.04; H, 5.08; N, 12.34.

4.1.18. Ethyl 4-(4-chlorophenyl)-6-methyl-2-(((5-phenyl-1,3,4-oxadiazol-2-yl)methyl)thio)-1,4-dihydropyrimidine-5-carboxylate (9r).

Yield: 89%; Melting point: 170-172 °C; IR (KBr) ν_{max}/cm^{-1} 3394, 3170, 1716,1693, 1654. ^{1}H NMR (400 MHz, DMSO-d_6) δ 10.78 (s, 1H, N<u>H</u>), 7.85 (d, *J* = 7.2 Hz, 2H, Ar-<u>H</u>), 7.55-7.38 (m, 7H, Ar-<u>H</u>), 6.15 (s, 1H, C4-<u>H</u>), 4.49 (d, *J* = 17.4 Hz, 1H, S-C<u>H</u>$_2$), 4.38 (d, *J* = 17.3 Hz, 1H, S-C<u>H</u>$_2$), 4.04 (q, *J* = 6.3 Hz, 2H, C<u>H</u>$_2$-CH$_3$), 2.37 (s, 3H, C6-C<u>H</u>$_3$), 1.12 (t, *J* = 7.1 Hz, 3H, CH$_2$-C<u>H</u>$_3$). ^{13}C NMR (100 MHz, DMSO-d_6+TFA) δ 167.62, 165.15, 164.55, 163.89, 163.57, 162.03, 160.34, 147.48, 143.43, 142.37, 138.91, 137.02, 134.36, 134.18, 133.34, 132.20, 132.02, 131.17, 129.34, 129.03, 128.85, 128.54, 128.41, 128.24, 126.64, 123.26, 106.69, 105.64, 61.03, 60.87, 56.64, 54.77, 30.99, 25.61, 17.39, 16.82, 13.64, 13.47. Anal. Calcd for $C_{23}H_{21}ClN_4O_3S$ (468.96):C, 58.91; H, 4.51; N, 11.95. Found: C, 59.18; H, 4.63; N, 12.32.

4.2. Biological evaluation

4.2.1. Preliminary in vitro anticancer screening [36]

The human tumor cell lines of the cancer screening panel are grown in RPMI 1640 medium containing 5% fetal bovine serum and 2 mM L-glutamine. For a typical screening experiment, cells are inoculated into 96 well microtiter plates in 100 µl at plating densities ranging from 5,000 to 40,000 cells/well depending on the doubling time of individual cell lines. After cell inoculation, the microtiter plates are incubated at 37° C, 5 % CO2, 95 % air and 100 % relative humidity for 24 h prior to addition of experimental drugs. After 24 h, two plates of each cell line are fixed *in situ* with TCA, to represent a measurement of the cell population for each cell line at the time of drug addition. Experimental drugs are solubilized in dimethyl sulfoxide at 400-fold the desired final maximum test concentration and stored frozen prior to use. At the time of drug addition, an aliquot of frozen concentrate is thawed and diluted to twice the desired final maximum test concentration with complete medium containing 50 µg/ml gentamicin. Aliquots of 100 µl of these different drug dilutions are added to the appropriate microtiter wells already containing 100 µl of medium, resulting in the required final drug concentrations 10 µM. Controls, containing only phosphate buffer saline and DMSO at identical dilutions, were prepared in the same manner. Following drug addition, the plates are incubated for an additional 48 h at 37°C, 5 % CO2, 95 % air, and 100 % relative humidity. For adherent cells, the assay is terminated by the addition of cold TCA. Cells are fixed *in situ* by the gentle addition of 50 µl of cold 50 % (w/v) TCA (final concentration, 10 % TCA) and incubated for 60 minutes at 4°C. The supernatant is discarded, and the plates are washed five times with tap water and air dried. Sulforhodamine B (SRB) solution (100 µl) at 0.4 % (w/v) in 1 % acetic acid is added to each well, and plates are incubated for 10 minutes at room temperature. After staining, unbound dye is removed by washing five times with 1 % acetic acid and the plates are air dried. Bound stain is subsequently solubilized with 10 mM trizma base, and the absorbance is read on an automated plate reader at a wavelength of 515 nm. For suspension cells, the methodology is the same except that the assay is terminated by fixing settled cells at the bottom of the wells by gently adding 50 µl of 80 % TCA (final concentration, 16 % TCA). Using the seven absorbance measurements, the percentage growth of the treated cells is calculated compared to the untreated control cells.

4.2.2. MTT assay for cell viability

HL-60(TB) and MOLT-4 cells were trypsinized and washed with Ca^{2+}/Mg^{2+} free PBS (pH 7.2). Cells were adjusted to 1.2-1.8 X 10^4 cells/ml with Dulbecco's Modified Eagle's Medium (DMEM) (Invitrogen Life Technologies) supplemented with 10% FBS (Hyclone, Logan, UT,USA), 10 µg/ml of insulin (Sigma), 1% penicillin/streptomycin and plated (100µl/well) in 96-well cell culture plate overnight at 37 °C with 5% CO_2 and 95% humidity. One hundred micro liters of serial 10-fold diluted sterile tested compounds were added to final concentrations of 0.01 - 100 µM. Culture medium was used as negative control. Cultures were incubated for 24h. Supernatants were discarded, 50µl/well of methylthiazolyldiphenyl-tetrazolium bromide (MTT) solution (5mg/ml in PBS, Sigma) was added and incubated for 4 h at 37°C with 5% CO_2. Acid-isopropanol (100 µl of 0.04 N HCI in isopropanol) was added to all wells and mixed thoroughly to dissolve the dark blue crystals. After a few minutes at room temperature to ensure that all crystals were dissolved. The absorbance were read on Robonik P2000 spectrophotometer at a wavelength of 490 nm and DMEM used as a blank control. Results from eight separate experiments were recorded and the percentage of viable cells was calculated.

4.2.3. DNA-flow cytometry analysis

HL-60(TB) cells at a density of 1×10^6 cells were exposed to 0.112 µM of **9m,** 0.294 µM of monastrol or to DMSO (0.002%), as a control for 24 h. Also, MOLT-4 cells at a density of 1×10^6 cells were exposed to 0.160 µM of **9n,** 0.430 µM of monastrol or DMSO (0.002%), as a control for 24 h. The cells were detached by trypsinization, washed in ice-cold PBS, fixed in ice cold 70% ethanol. Keep the cells in ethanol for at least 2h at 4°C then harvested by centrifugation. Subsequently, cells were washed in PBS and then stained using Cycle TEST™ plus DNA Reagent Kit (ab139418_Propidium Iodide Flow Cytometry Kit) (Becton Dickinson Biosciences, San Jose, CA, USA). Cell cycle distribution was determined using a FACSCalibur flow cytometer (Becton Dickinson Biosciences, San Jose, CA, USA) and analyzed using Cell Quest software (Becton Dickinson).

4.2.4. Annexin V-FITC apoptosis assay

Apoptotic cells were analyzed by the Annexin V-FITC Apoptosis Detection Kit (BD Biosciences, USA). HL-60(TB) cells were cultured and incubated for 24 h in the presence of 0.112 µM of **9m,** 0.294 µM of monastrol or DMSO (0.002%), as a

control. Also, MOLT-4 cells were cultured in the same manner in the presence of 0.160 µM of **9n,** 0.430 µM of monastrol or DMSO (0.002%), as a control and incubated for 24 h. Cells were collected, washed twice with PBS, and centrifuged. Thereafter, 1×10^6 cells/ml were stained with a combination of fluorescein isothiocyanate (FITC), annexin V and propidium iodide (PI) and The reaction was allowed to proceed in the dark for 30 min at room temperature then analyzed by flow cytometry on FACSCalibur (BD Biosciences, San Jose, CA, USA) without gating restrictions using 10,000 cells. Quadrant analysis of co-ordinate dot plots was performed with Cell Quest software. Unstained cells were used to adjust the photomultiplier voltage and for compensation setting adjustment in order to eliminate spectral overlap between the FL1 and FL2 signals.

4.2.5. Docking study

A docking study was carried out using Molecular Operating Environment (MOE version 2008.10) [33]. For this purpose, the crystal structure of kinesin Eg5 with the allosteric inhibitor monastrol (PDB ID code 1Q0B) [32] was obtained from the Protein Data Bank in order to prepare the protein for docking studies. The docking procedure was followed using the standard protocol implemented in MOE 2008.10 and the geometry of the resulting complexes was studied using MOE's Pose Viewer utility. The enzyme was prepared for docking as follows: 1) the co-crystallized ligand and water molecules were removed. 2) The enzyme was 3D protonated, where hydrogen atoms were added at their standard geometry, the partial charges were computed and the system was optimized. Flexible ligand–rigid receptor docking of the most stable conformers was done with MOE-DOCK using pharmacophore as the placement method and London dG as the scoring function. The obtained poses were subjected to forcefield refinement using the same scoring function. Thirty of the most stable docking models for each ligand were retained with the best scored conformation.

References:

[1] T.U. Mayer, T.M. Kapoor, S.J. Haggarty, R.W. King, S.L. Schreiber, T.J. Mitchison, Small molecule inhibitor of mitotic spindle bipolarity identified in a phenotype-based screen, Science, 286 (1999) 971-974.

[2] I. Leizerman, R. Avunie-Masala, M. Elkabets, A. Fich, L. Gheber, Differential effects of monastrol in two human cell lines, Cellular and Molecular Life Sciences CMLS, 61 (2004) 2060-2070.

[3] G. Cavaletti, E. Cavalletti, P. Montaguti, N. Oggioni, O. De Negri, G. Tredici, Effect on the peripheral nervous system of the short-term intravenous administration of paclitaxel in the rat, Neurotoxicology, 18 (1996) 137-145.

[4] S.A. Haque, T.P. Hasaka, A.D. Brooks, P.V. Lobanov, P.W. Baas, Monastrol, a prototype anti-cancer drug that inhibits a mitotic kinesin, induces rapid bursts of axonal outgrowth from cultured postmitotic neurons, Cell Motil. Cytoskeleton, 58 (2004) 10-16.

[5] E. Klein, S. DeBonis, B. Thiede, D.A. Skoufias, F. Kozielski, L. Lebeau, New chemical tools for investigating human mitotic kinesin Eg5, Bioorg. Med. Chem., 15 (2007) 6474-6488.

[6] B.P. Kumar, G. Sankar, R.N. Baig, S. Chandrashekaran, Novel Biginelli dihydropyrimidines with potential anticancer activity: a parallel synthesis and CoMSIA study, Eur. J. Med. Chem., 44 (2009) 4192-4198.

[7] A. Kamal, M.S. Malik, S. Bajee, S. Azeeza, S. Faazil, S. Ramakrishna, V. Naidu, M. Vishnuwardhan, Synthesis and biological evaluation of conformationally flexible as well as restricted dimers of monastrol and related dihydropyrimidones, Eur. J. Med. Chem., 46 (2011) 3274-3281.

[8] D.L. da Silva, F.S. Reis, D.R. Muniz, A.L.T. Ruiz, J.E. de Carvalho, A.A. Sabino, L.V. Modolo, Â. de Fátima, Free radical scavenging and antiproliferative properties of Biginelli adducts, Bioorg. Med. Chem., 20 (2012) 2645-2650.

[9] M. Gartner, N. Sunder-Plassmann, J. Seiler, M. Utz, I. Vernos, T. Surrey, A. Giannis, Development and biological evaluation of potent and specific inhibitors of mitotic Kinesin Eg5, ChemBioChem, 6 (2005) 1173-1177.

[10] V. Sarli, S. Huemmer, N. Sunder-Plassmann, T.U. Mayer, A. Giannis, Synthesis and biological evaluation of novel EG5 inhibitors, ChemBioChem, 6 (2005).

[11] H.Y.K. Kaan, V. Ulaganathan, O. Rath, H. Prokopcová, D. Dallinger, C.O. Kappe, F. Kozielski, Structural basis for inhibition of Eg5 by dihydropyrimidines: stereoselectivity of antimitotic inhibitors enastron, dimethylenastron and fluorastrol, J. Med. Chem., 53 (2010) 5676-5683.

[12] I. Garcia-Saez, S. DeBonis, R. Lopez, F. Trucco, B. Rousseau, P. Thuéry, F. Kozielski, Structure of human Eg5 in complex with a new monastrol-based inhibitor bound in the R configuration, J. Biol. Chem., 282 (2007) 9740-9747.

[13] K.V. Sashidhara, S.R. Avula, K. Sharma, G.R. Palnati, S.R. Bathula, Discovery of coumarin–monastrol hybrid as potential antibreast tumor-specific agent, Eur. J. Med. Chem., 60 (2013) 120-127.

[14] B. Yadagiri, S. Gurrala, R. Bantu, L. Nagarapu, S. Polepalli, G. Srujana, N. Jain, Synthesis and evaluation of benzosuberone embedded with 1, 3, 4-oxadiazole, 1, 3, 4-thiadiazole and 1, 2, 4-triazole moieties as new potential anti proliferative agents, Bioorg. Med. Chem. Lett., 25 (2015) 2220-2224.

[15] S. Valente, D. Trisciuoglio, T. De Luca, A. Nebbioso, D. Labella, A. Lenoci, C. Bigogno, G. Dondio, M. Miceli, G. Brosch, 1, 3, 4-Oxadiazole-containing histone deacetylase inhibitors: anticancer activities in cancer cells, J. Med. Chem., 57 (2014) 6259-6265.

[16] M.M.G. El-Din, M.I. El-Gamal, M.S. Abdel-Maksoud, K.H. Yoo, C.-H. Oh, Synthesis and in vitro antiproliferative activity of new 1, 3, 4-oxadiazole derivatives possessing sulfonamide moiety, Eur. J. Med. Chem., 90 (2015) 45-52.

[17] X. Zheng, Z. Li, Y. Wang, W. Chen, Q. Huang, C. Liu, G. Song, Syntheses and insecticidal activities of novel 2, 5-disubstituted 1, 3, 4-oxadiazoles, J. Fluorine Chem., 123 (2003) 163-169.

[18] M. Moise, V. Sunel, L. Profire, M. Popa, J. Desbrieres, C. Peptu, Synthesis and biological activity of some new 1, 3, 4-thiadiazole and 1, 2, 4-triazole compounds containing a phenylalanine moiety, Molecules, 14 (2009) 2621-2631.

[19] W. Shi, X. Qian, R. Zhang, G. Song, Synthesis and quantitative structure-activity relationships of new 2, 5-disubstituted-1, 3, 4-oxadiazoles, J. Agric. Food Chem., 49 (2001) 124-130.

[20] M. Amir, K. Shikha, Synthesis and anti-inflammatory, analgesic, ulcerogenic and lipid peroxidation activities of some new 2-[(2, 6-dichloroanilino) phenyl] acetic acid derivatives, Eur. J. Med. Chem., 39 (2004) 535-545.

[21] S. Cao, X. Qian, G. Song, B. Chai, Z. Jiang, Synthesis and antifeedant activity of new oxadiazolyl 3 (2 H)-pyridazinones, J. Agric. Food Chem., 51 (2003) 152-155.

[22] V. Padmavathi, G.D. Reddy, S.N. Reddy, K. Mahesh, Synthesis and biological activity of 2-(bis ((1, 3, 4-oxadiazolyl/1, 3, 4-thiadiazolyl) methylthio) methylene) malononitriles, Eur. J. Med. Chem., 46 (2011) 1367-1373.

[23] P. Biginelli, Aldehyde-urea derivatives of aceto-and oxaloacetic acids, Gazz. Chim. Ital, 23 (1893) 360-413.

[24] C.O. Kappe, 100 years of the Biginelli dihydropyrimidine synthesis, Tetrahedron, 49 (1993) 6937-6963.

[25] A. Weis, Z. Porat, Z. Luz, Dihydropyrimidines, part 5. Dynamic NMR investigation of the annular tautomerism in dihydropyrimidines, J. Am. Chem. Soc., 106 (1984) 8021-8024.

[26] C. Kashima, M. Shimizu, Y. Omote, The tautomeric study in 2-substituted 1, 6-dihydro-4, 6, 6-trimethyl-pyrimidine systems, Tetrahedron Lett., 26 (1985) 5057-5060.

[27] H. Cho, T. Iwashita, M. Ueda, A. Mizuno, K. Mizukawa, M. Hamaguchi, On the tautomerism of dihydropyrimidines: the influence of the 2-and 5-substituents on the observation of tautomers, J. Am. Chem. Soc., 110 (1988) 4832-4834.

[28] J.A. DaSilva, C. Barríab, C. Jullianb, P. Navarreteb, L. NúñezVergaraa, J. Squellaa, Unexpected diastereotopic behaviour in the 1H NMR spectrum of 1, 4-dihydropyridine derivatives triggered by chiral and prochiralcentres, J. Braz. Chem. Soc., 16 (2005) 112.

[29] H.R. Memarian, F. Rezaie, H. Sabzyan, M. Ranjbar, Substituent effect on the tautomerism of 5-acetyl-2-methoxydihydropyrimidines: experimental NMR and computational DFT studies, J. IRAN. CHEM. SOC, 11 (2014) 1265-1274.

[30] T. Mosmann, Rapid colorimetric assay for cellular growth and survival: application to proliferation and cytotoxicity assays, J. Immunol. Methods, 65 (1983) 55-63.

[31] Molinspiration Cheminformatics (http://www.molinspiration.com/cgi-bin/properties).

[32] Y. Yan, V. Sardana, B. Xu, C. Homnick, W. Halczenko, C.A. Buser, M. Schaber, G.D. Hartman, H.E. Huber, L.C. Kuo, Inhibition of a mitotic motor protein: where, how, and conformational consequences, J. Mol. Biol., 335 (2004) 547-554.

[33] Molecular Operating Environment (MOE), Version 2008. 10, Chemical Computing Group, Inc. Montreal, Quebec, Canada. http://www.chemcomp.com.

[34] M.S. Mohamed, A. Mohamed, Z. Mohamed, Z.M. Mohamed, New Theopyrimidine Derivatives of Expected Anti inflammatory Activity, Pharmacophore, 3 (2012) 62-75.

[35] A. Wang, X. Liu, Z. Su, H. Jing, New magnetic nanocomposites of ZrO 2–Al 2 O 3–Fe 3 O 4 as green solid acid catalysts in organic reactions, Catal. Sci. Technol., 4 (2014) 71-80.

[36] P. Skehan, R. Storeng, D. Scudiero, A. Monks, J. McMahon, D. Vistica, J.T. Warren, H. Bokesch, S. Kenney, M.R. Boyd, New colorimetric cytotoxicity assay for anticancer-drug screening, J. Natl. Cancer Inst., 82 (1990) 1107-1112.

Table 1: Percentage growth inhibition (GI %) of in vitro subpanel tumor cell lines at 10 μM concentration of the selected compounds

Subpanel cancer cell Lines	% Growth Inhibition (GI %)[a]												
	9b	**9c**	**9e**	**9f**	**9g**	**9h**	**9i**	**9j**	**9k**	**9m**	**9n**	**9o**	**9q**
Leukemia													
CCRF-CEM	-	20.86	15.72	11.86	12.41	16.90	**60.26**	12.91	**56.59**	**38.24**	**72.75**	15.35	14.14
HL-60(TB)	11.46	**40.27**	15.19	19.19	37.98	23.54	**78.56**	-	**77.47**	**80.42**	**106.39**	11.98	25.23
K-562	-	11.06	-	-	25.18	14.37	**44.25**	-	39.28	27.47	nt	-	14.71
MOLT-4	-	24.38	10.94	-	31.29	20.43	**92.98**	-	**91.71**	**44.97**	**88.75**	-	21.58
RPMI-8226	13.78	32.90	14.04	16.28	27.31	25.84	**64.22**	18.28	**61.64**	**46.38**	nt	-	27.18
SR	19.06	37.79	13.33	19.06	24.95	16.66	**57.11**	18.07	**61.18**	16.40	**62.06**	15.94	26.48
Non-small cell lung cancer													
A549/ATCC	-	21.43	15.59	-	28.98	11.65	31.03	11.47	37.63	29.49	**46.55**	12.73	17.30
EKVX	-	-	-	-	14.78	-	19.85	-	28.70	-	22.77	-	-
HOP-62	-	11.59	19.35	-	27.83	-	-	-	13.11	25.10	17.48	12.02	-
HOP-92	-	26.49	16.54	-	**40.14**	27.82	35.92	17.56	**42.20**	**48.97**	**73.64**	21.41	37.02
NCI-H226	11.55	11.45	-	10.38	11.43	10.62	30.13	11.80	21.10	-	20.97	10.43	10.11
NCI-H23	-	-	-	-	-	-	21.21	-	24.28	-	33.95	-	-
NCI-H322M	-	11.96	-	-	-	-	17.66	-	13.56	-	21.12	-	10.32
NCI-H460	-	-	-	-	-	-	21.05	-	19.58	-	**40.76**	-	-
NCI-H522	15.59	20.91	17.98	14.06	**54.12**	17.47	31.06	-	32.44	**74.59**	**49.82**	26.46	22.44
Colon cancer													
COLO 205	-	-	-	-	10.43	-	20.44	-	22.39	29.56	nt	-	-
HCC-2998	-	-	-	-	-	-	20.09	-	-	10.31	15.54	-	-
HCT-116	13.10	25.75	-	-	36.75	21.67	**53.81**	-	**51.36**	**56.51**	**71.24**	-	18.61
HCT-15	-	11.02	-	-	21.77	15.78	32.40	-	34.91	29.54	**44.67**	-	11.34
HT29	-	-	-	-	22.34	10.31	24.77	-	21.28	**46.44**	**46.90**	-	12.44
KM12	-	-	-	-	10.32	-	30.34	-	23.97	15.98	36.59	-	-
SW-620	-	-	-	-	-	-	14.08	-	-	-	33.77	-	-
CNS cancer													
SF-268	-	-	-	-	-	-	14.02	-	13.34	-	26.67	-	-
SF-295	-	-	-	-	23.41	-	25.89	-	26.44	25.46	**52.77**	-	12.12
SF-539	-	-	-	-	-	-	12.27	-	11.33	-	13.64	-	-
SNB-19	-	16.63	13.41	-	11.69	11.64	27.01	12.46	28.03	10.36	27.06	11.42	10.14
SNB-75	16.81	28.09	17.32	-	-	-	26.28	18.85	32.31	16.82	15.90	17.53	13.80
U251	-	14.75	15.34	-	21.19	10.10	26.13	10.11	34.26	-	34.72	-	15.05
Melanoma													
LOX IMVI	-	-	-	-	11.11	-	23.14	-	25.05	17.70	**41.74**	-	-
MALME-3M	-	11.59	12.35	-	-	-	18.32	-	16.93	-	27.21	-	-
M14	-	-	13.44	-	19.50	-	30.70	-	26.03	26.23	34.81	-	-
MDA-MB-435	-	-	-	-	-	-	30.41	-	34.94	-	30.97	-	-
SK-MEL-2	-	-	-	-	34.49	-	-	-	-	**39.92**	**39.96**	-	-

SK-MEL-28	-	-	-	L	-	-	20.17	-	18.71	-	-	-	-
SK-MEL-5	-	-	-	-	-	12.47	**59.11**	-	**48.61**	-	19.72	-	14.52
UACC-257	-	-	-	-	25.90	-	13.06	-	27.00	22.19	31.92	11.82	-
UACC-62	22.65	27.72	10.80	15.37	34.86	10.72	**50.13**	15.28	**44.70**	26.55	**48.43**	-	17.05
Ovarian cancer													
IGROV1	15.40	23.39	-	10.96	-	17.14	37.71	17.80	34.55	14.57	**56.12**	-	13.94
OVCAR-3	-	-	-	-	-	-	29.21	-	22.52	17.27	37.17	-	-
OVCAR-4	-	-	12.15	-	-	-	29.97	-	30.44	16.90	**47.27**	-	-
OVCAR-5	-	-	-	10.44	-	-	10.36	-	-	10.46	10.99	-	-
OVCAR-8	-	14.50	-	-	20.40	11.68	25.22	-	27.29	33.66	**45.78**	-	17.83
NCI/ADR-RES	-	-	-	-	-	-	30.11	-	32.47	21.28	**45.36**	-	-
SK-OV-3	-	-	18.32	-	25.65	-	17.40	-	17.97	29.89	-	14.16	-
Renal cancer													
786-0	16.45	12.60	-	15.43	31.37	10.65	16.59	18.77	15.12	**43.05**	34.81	-	20.25
A498	-	-	-	-	-	12.30	19.26	-	26.84	-	22.28	-	-
ACHN	-	13.52	-	-	-	-	35.91	-	30.28	-	**42.28**	-	18.97
CAKI-1	16.90	21.07	29.93	11.99	22.29	17.50	38.39	17.80	32.79	35.15	nt	24.85	24.69
RXF 393	-	-	-	-	-	-	32.30	-	25.02	-	**56.62**	14.49	-
SN12C	-	12.96	-	-	14.75	-	-	-	-	-	34.63	-	19.87
TK-10	14.57	13.06	-	14.37	30.79	13.90	22.48	-	20.09	30.29	20.65	-	28.35
UO-31	26.15	43.64	29.70	16.36	19.39	22.21	**51.33**	20.31	**47.61**	35.91	**62.80**	21.73	-
Prostate cancer													
PC-3	18.54	31.07	18.71	14.65	**42.25**	23.42	**51.24**	17.95	**51.21**	**39.17**	**54.90**	12.47	26.79
DU-145	-	-	-	-	-	-	12.85	-	15.73	13.49	26.88	-	-
Breast cancer													
MCF7	10.61	16.39	10.52	-	18.23	13.30	**51.01**	-	**55.17**	31.98	**68.03**	-	14.04
MDA-MB-231/ATCC	17.04	27.00	14.36	-	-	-	37.29	10.22	**40.23**	18.93	**58.31**	-	14.66
HS 578T	-	-	-	-	-	-	16.33	-	12.87	-	32.90	-	-
BT-549	-	15.07	-	13.94	**42.66**	-	24.70	16.90	20.24	**46.85**	10.30	-	12.76
T-47D	24.09	39.49	28.87	25.59	**53.79**	27.10	**50.15**	15.16	**52.02**	**69.24**	**52.64**	33.30	32.56
MDA-MB-468	11.27	10.76	-	-	14.67	17.07	**51.05**	-	**41.80**	-	11.59	-	18.07

[a] -, GI <10%; nt, not tested; L, compound proved lethal to the cancer cell line.

Table 2: IC_{50} againest HL-60(TB) and MOLT-4 cancer cell lines

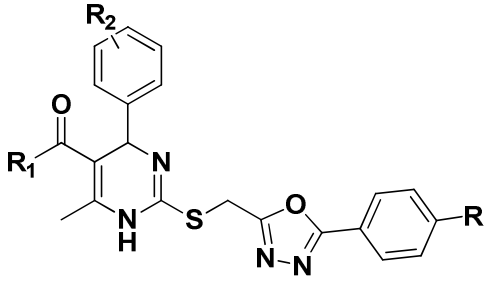

9i-r

Compound	R	R^1	R^2	IC_{50} μm ± SE[a]		log P
				HL-60(TB)	MOLT-4	
9i	Cl	OC_2H_5	4-Cl	0.103 ± 0.017	0.623 ± 0.010	5.53
9k	Cl	OC_2H_5	4-Br	0.143 ± 0.015	0.086 ± 0.007	5.66
9l	Cl	OC_2H_5	2-Cl	193 ± 5.39	255 ± 6.01	5.48
9m	Cl	OC_2H_5	3-Cl	0.056 ± 0.007	1.788 ± 0.009	5.51
9n	Cl	OC_2H_5	2,4-diCl	0.153 ± 0.021	0.080 ± 0.017	6.14
9p	CH_3	OC_2H_5	4-Cl	220 ± 6.53	538 ± 7,46	5.30
9r	H	OC_2H_5	4-Cl	74.4 ± 4.17	344 ± 8.09	4.85
monastrol	–	–	–	0.147 ± 0.008	0.215 ± 0.013	–

[a] IC_{50} values are the mean ± S.E. of eight separate experiments

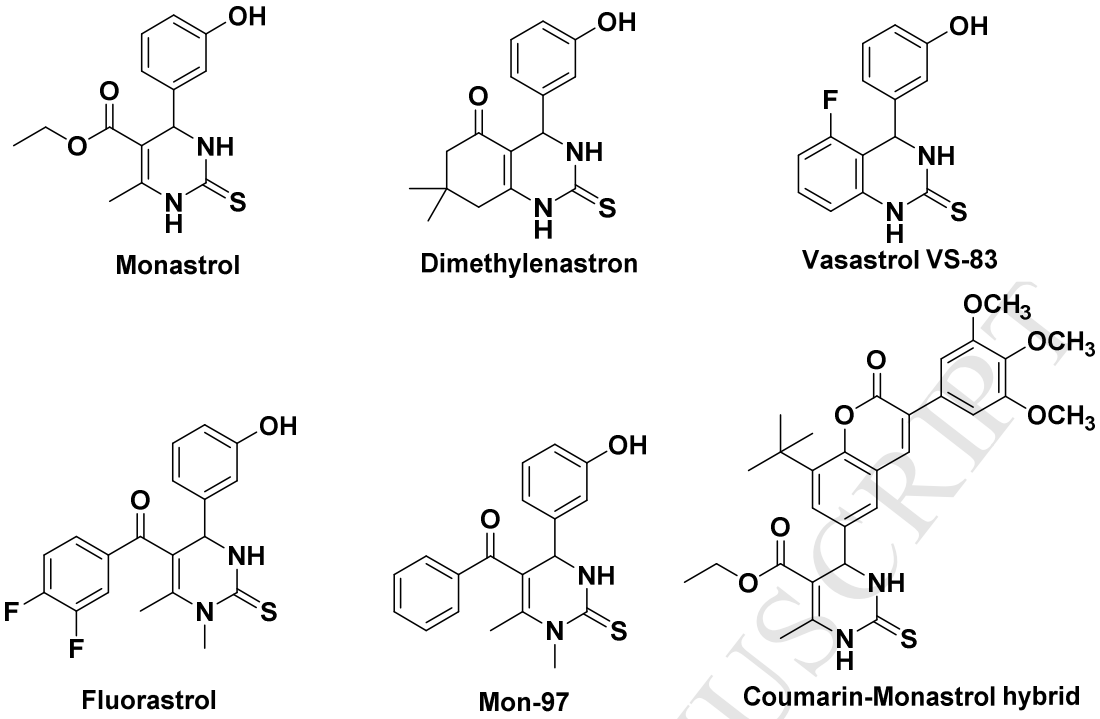

Figure 1: Examples of some DHPM-based anticancer agents

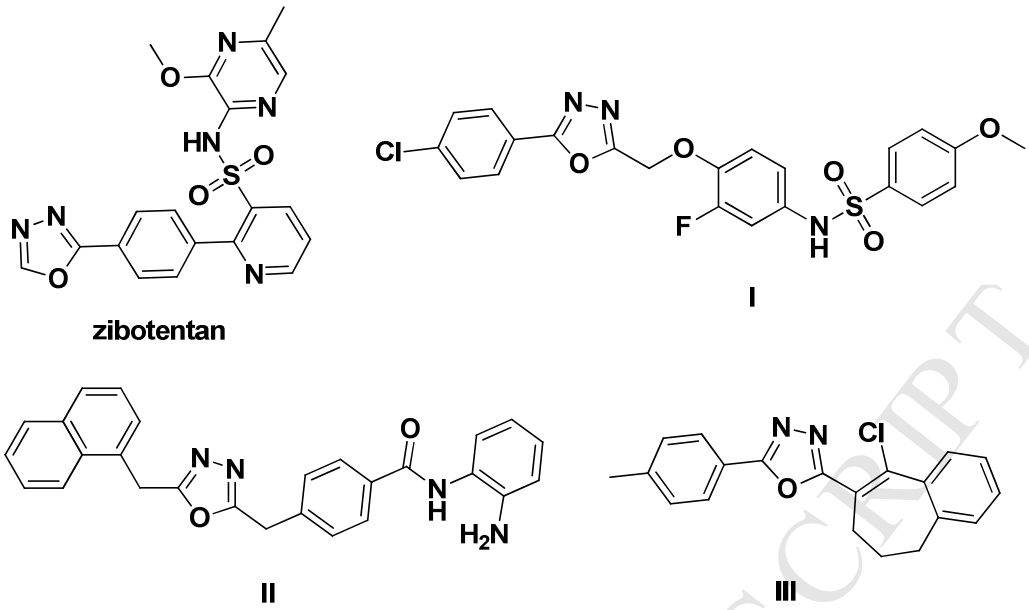

Figure 2: Examples of some 1,3,4-oxadiazole-based anticancer agents

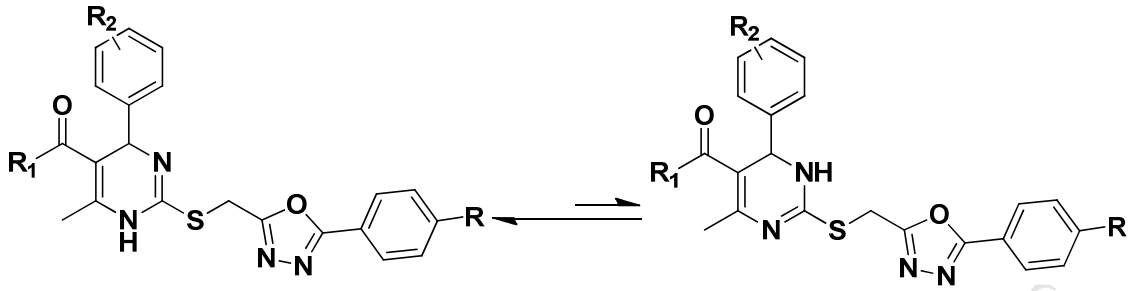

Figure 3: Possible tautomerism of dihydropyrimidine derivatives.

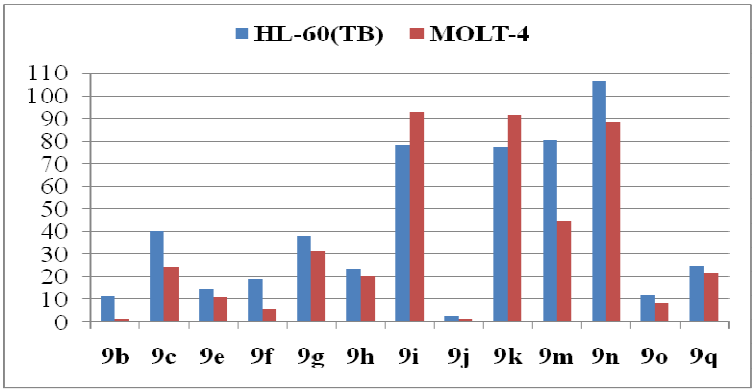

Figure 4: Inhibitory effects of the tested compounds at 10 µM concentration against Leukemia HL-60(TB) and MOLT-4 cell lines.

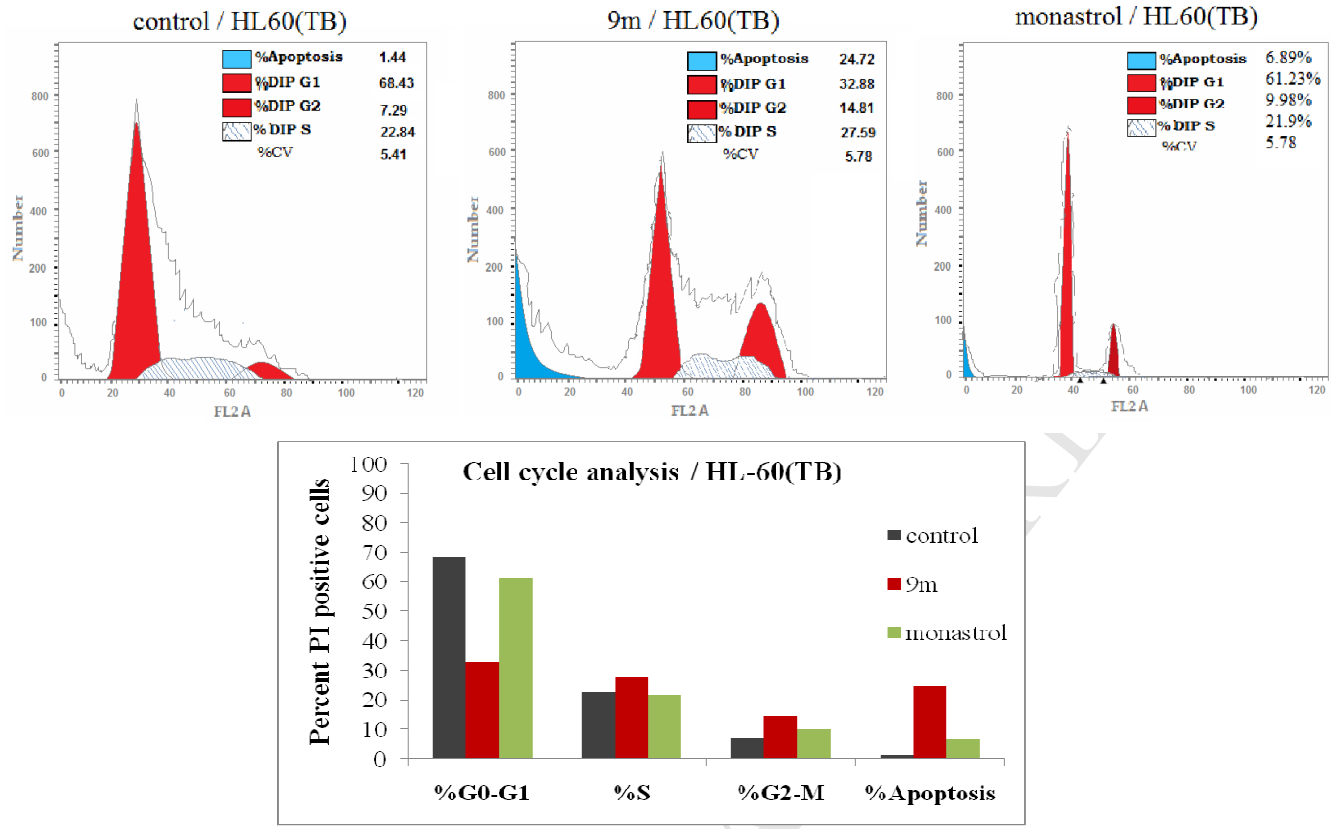

Figure 5: Effect of monastrol and **9m** on DNA-ploidy flow cytometric analysis of HL-60(TB) cells. The cells were treated with DMSO as control, monastrol or **9m** for 24 h.

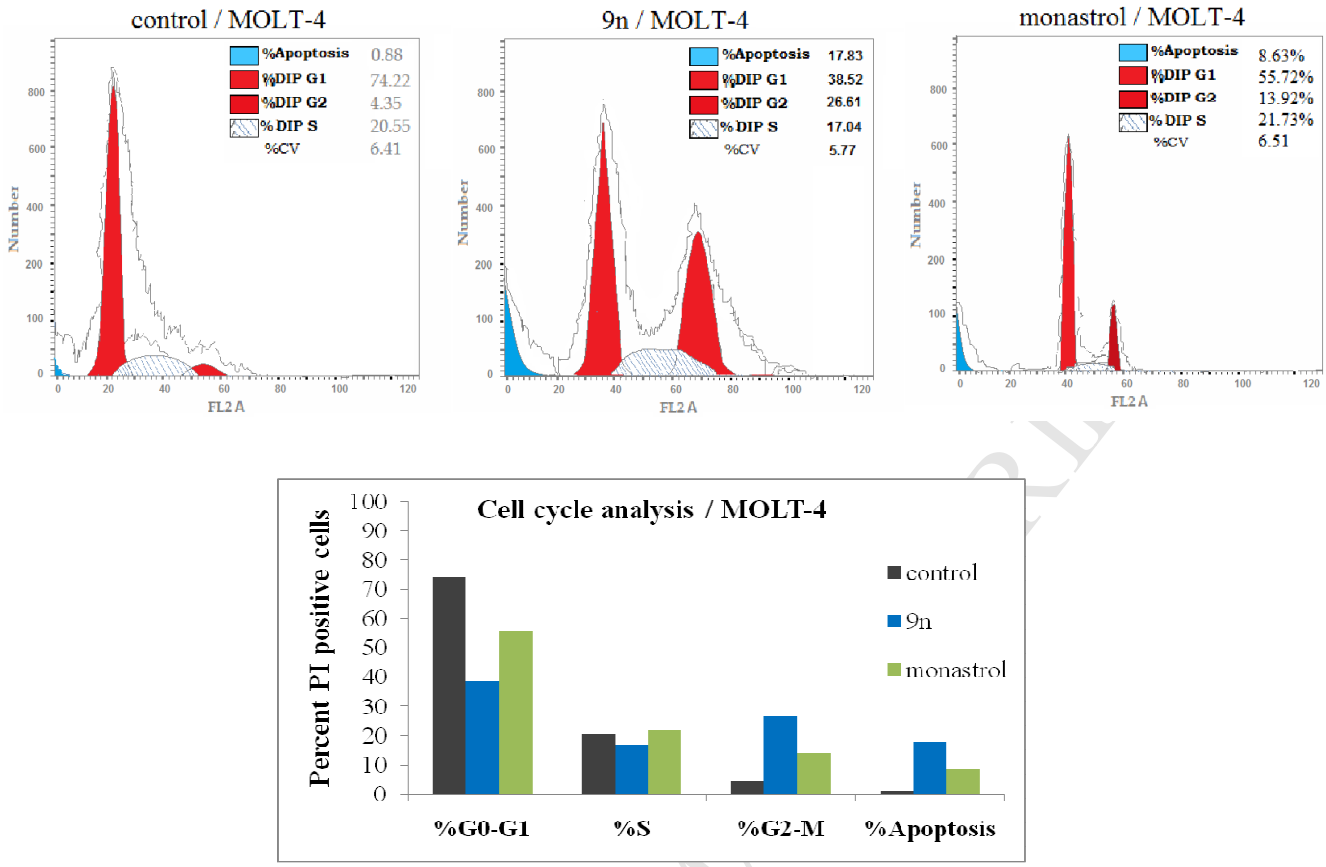

Figure 6: Effect of monastrol and **9n** on DNA-ploidy flow cytometric analysis of MOLT-4 cells. The cells were treated with DMSO as control, monastrol or **9n** for 24 h.

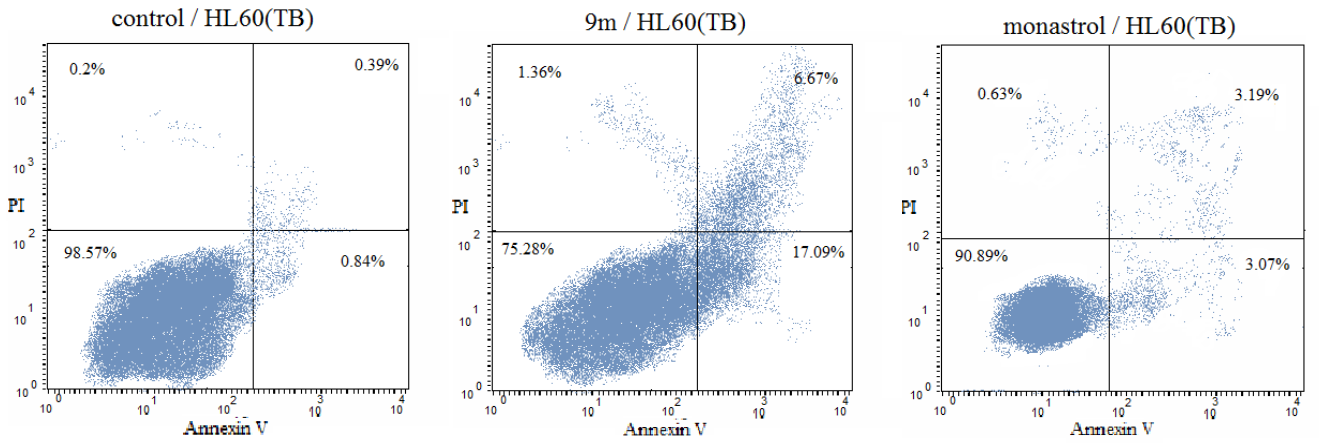

Figure 7: Effect of monastrol and **9m** on the percentage of annexin V-FITC-positive staining in HL-60(TB) cells. The cells were treated with DMSO as control, monastrol or **9m** for 24 h.

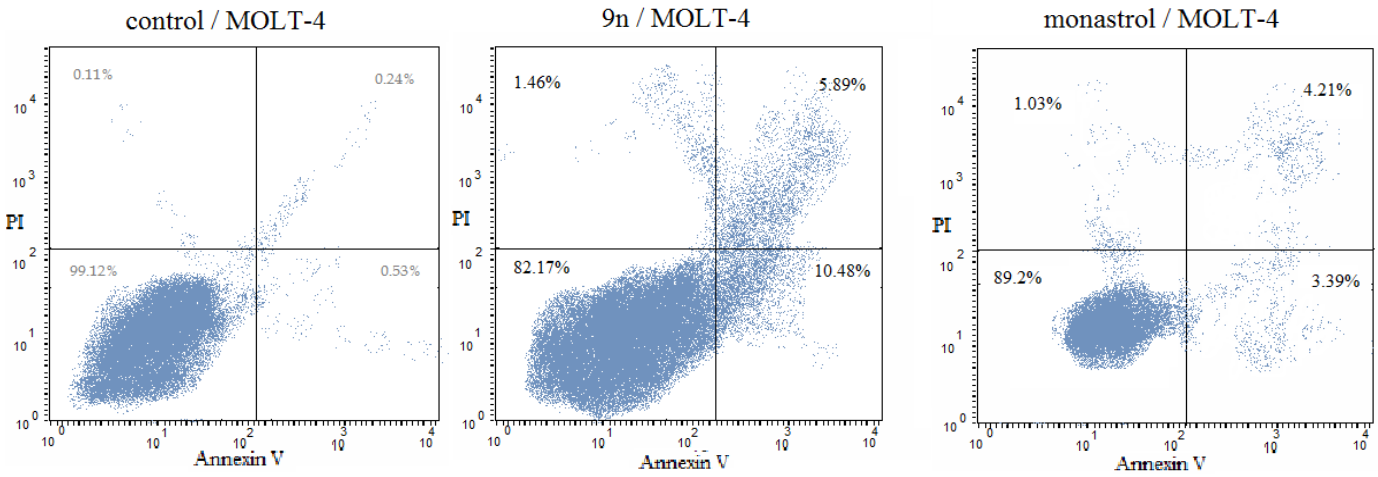

Figure 8: Effect of monastrol and **9n** on the percentage of annexin V-FITC-positive staining in MOLT-4 cells. The cells were treated with DMSO as control, monastrol or **9n** for 24 h.

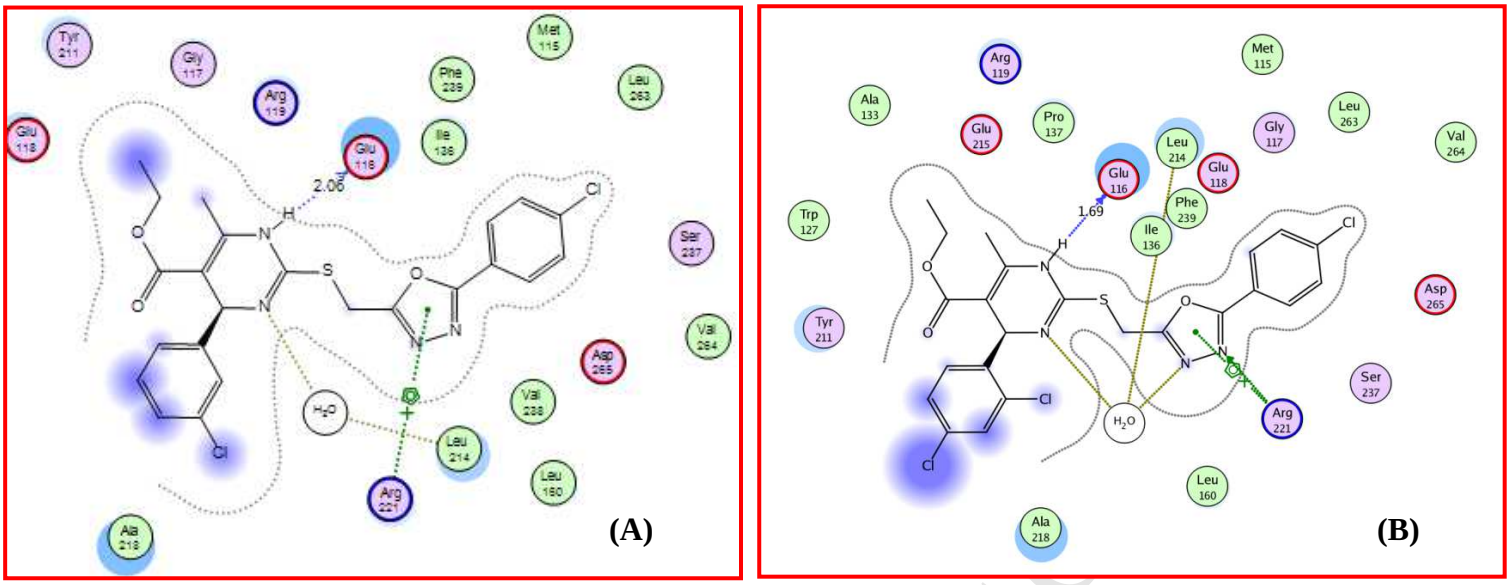

Figure 9: 2D diagram representation of compounds **9m** (A) and **9n** (B) showing their interaction with the motor domain of Eg5 allosteric binding site.

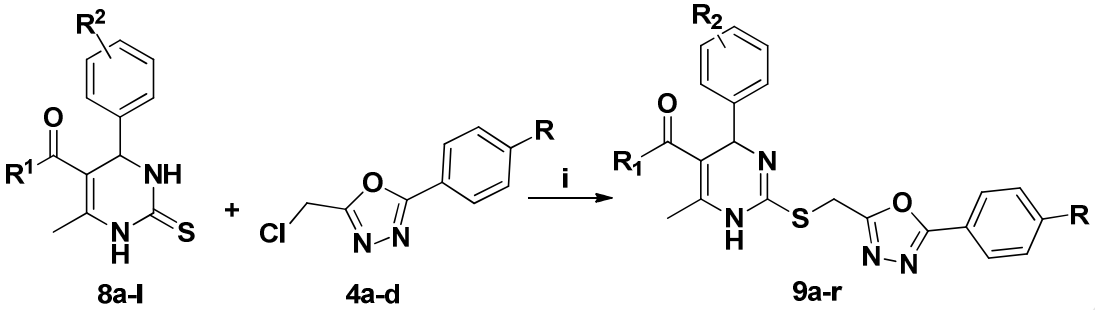

9a: R = Cl, $R^1 = CH_3$, R^2 = H
9b: R = Cl, $R^1 = CH_3$, R^2 = 4-F
9c: R = Cl, $R^1 = CH_3$, R^2 = 4-Cl
9d: R = Cl, $R^1 = CH_3$, R^2 = 4-OCH_3
9e: R = OCH_3, $R^1 = CH_3$, R^2 = 4-F
9f: R = CH_3, $R^1 = CH_3$, R^2 = 4-F
9g: R = Cl, $R^1 = OC_2H_5$, R^2 = H
9h: R = Cl, $R^1 = OC_2H_5$, R^2 = 4-F
9i: R = Cl, $R^1 = OC_2H_5$, R^2 = 4-Cl
9j: R = Cl, $R^1 = OC_2H_5$, R^2 = 4-OCH_3
9k: R = Cl, $R^1 = OC_2H_5$, R^2 = 4-Br
9l: R = Cl, $R^1 = OC_2H_5$, R^2 = 2-Cl
9m: R = Cl, $R^1 = OC_2H_5$, R^2 = 3-Cl
9n: R = Cl, $R^1 = OC_2H_5$, R^2 = 2,4-diCl
9o: R = OCH_3, $R^1 = OC_2H_5$, R^2 = 4-F
9p: R = CH_3, $R^1 = OC_2H_5$, R^2 = 4-Cl
9q: R = CH_3, $R^1 = OC_2H_5$, R^2 = 4-F
9r: R = H, $R^1 = OC_2H_5$, R^2 = 4-Cl

Scheme 1: Synthetic pathway of compounds **9a-r**.

Reagents and conditions: (i) TEA / EtOH / KI /reflux.

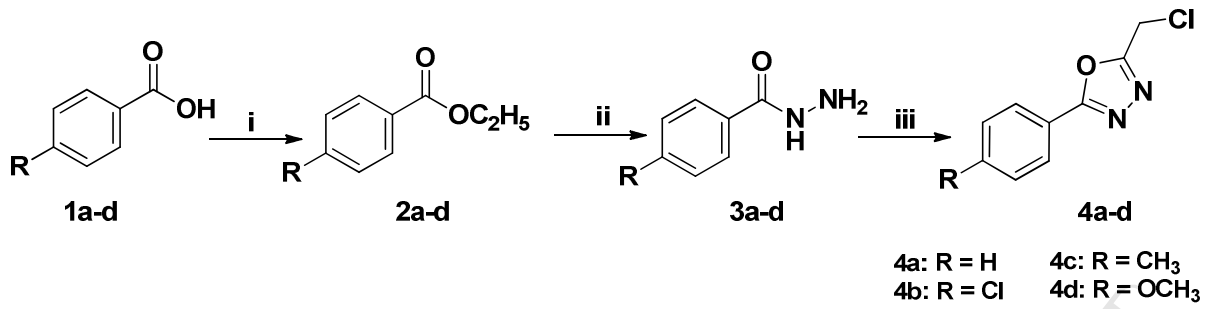

Scheme 2: Synthesis of 2-(chloromethyl)-5-aryl-1,3,4-oxadiazole derivatives **4a-d**.

Reagents and conditions: (i) EtOH / conc H_2SO_4 / reflux (ii) $NH_2NH_2.H_2O$ / EtOH / reflux (iii) Monochloroacetic acid / $POCl_3$ / reflux.

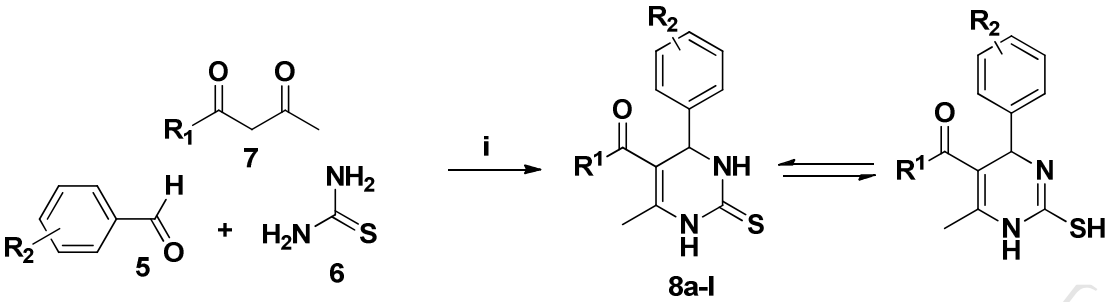

8a: $R^1 = CH_3$, R^2 = H
8b: $R^1 = CH_3$, R^2 = 4-F
8c: $R^1 = CH_3$, R^2 = 4-Cl
8d: $R^1 = CH_3$, R^2 = 4-OCH_3
8e: $R^1 = OC_2H_5$, R^2 = H
8f: $R^1 = OC_2H_5$, R^2 = 4-F
8g: $R^1 = OC_2H_5$, R^2 = 4-Cl
8h: $R^1 = OC_2H_5$, R^2 = 4-OCH_3
8i: $R^1 = OC_2H_5$, R^2 = 4-Br
8j: $R^1 = OC_2H_5$, R^2 = 2-Cl
8k: $R^1 = OC_2H_5$, R^2 = 3-Cl
8l: $R^1 = OC_2H_5$, R^2 = 2.4-di-Cl

Scheme 3: Synthetic pathway of 6-methyl-4-aryl-1,2,3,4-tetrahydropyrimidin 2(1*H*)-thione derivatives **8a-l**. Reagents and conditions: (i) HCl / EtOH / reflux

Design, synthesis and anticancer activity of new monastrol analogues bearing 1,3,4-oxadiazole moiety

Highlights

- A series of dihydropyrimidine (DHPM) compounds bearing 1,3,4-oxadiazole moiety was designed and synthesized as monastrol analogues.
- Thirteen compounds were subjected to in vitro NCI antitumor screening at a single dose of 10 μM concentration
- Seven compounds were IC_{50} evaluated against leukemia HL-60(TB) and MOLT-4 cancer cell lines.
- Four compounds showed potent activity against HL-60(TB) and MOLT-4 comparable to monastrol.